THE SPECTRAL THEORY OF ADIABATIC QUASI-PERIODIC OPERATORS ON THE REAL LINE

ALEXANDER FEDOTOV AND FRÉDÉRIC KLOPP

This paper is dedicated to L. Pastur on the occasion of his 65th birthday.

Abstract. In this paper, we present a review of our recent results on spectral properties of adiabatic quasi-periodic Schrödinger equations. We describe new spectral phenomena and explain them in terms of simple semi-classical heuristics.

Résumé. Cet article présente certains de nos résultats récents sur des propriétés spectrales des équations de Schrödinger quasi-périodiques. Nous décrivons de nouveaux phénomènes spectraux et les interprétons grâce à une heuristique semi-classique

0. Introduction

The purpose of this paper is to present recent results on the spectral theory of the following family of differential equations

$$H_{z,\varepsilon}\psi = -\frac{d^2}{dx^2}\psi(x) + [V(x-z) + W(\varepsilon x)]\psi(x) = E\psi(x), \quad x \in \mathbb{R}, \tag{0.1}$$

where

(H):
- $W(z) = \alpha\cos(z)$, $\alpha > 0$,
- V is a non constant 1-periodic function in $L^2_{\mathrm{loc}}(\mathbb{R})$,
- ε is fixed positive number,
- z is a real parameter indexing the equations of the family.

Our study is done in the adiabatic limit i.e. when ε tends to 0. This means that the potential V is oscillating at speed 1 and the potential $W(\varepsilon\cdot)$ is oscillating very slowly at speed $\varepsilon/2\pi$.

When studying the nature of the spectrum, we pick ε so that $2\pi/\varepsilon$ be irrational. In this case, the potential $V(\cdot - z) + W(\varepsilon\cdot)$ becomes quasi-periodic. Quasi-periodic equations have been intensively studied during the last 30 years (see e.g. [17, 20]) and they are suspected (and in some rare cases known) to have very peculiar spectral characteristics (Cantor spectrum, spectral transitions, etc).

The results we describe were obtained in [13, 12, 10, 7, 11]. The object central to our study is the monodromy matrix that we describe now.

0.1. **The monodromy matrix.** Consider a consistent basis $(\psi_{1,2})$ i.e. a basis of solutions of (0.1) whose Wronskian is independent of z and that are 1-periodic in z i.e.

$$\psi_{1,2}(x,\, z+1) = \psi_{1,2}(x,\, z), \quad \forall x, z. \tag{0.2}$$

The functions $\psi_{1,2}(x + 2\pi/\varepsilon, z + 2\pi/\varepsilon)$ being solutions of equation (0.1), one can write

$$\Psi\left(x + 2\pi/\varepsilon, z + 2\pi/\varepsilon\right) = M\left(z\right)\Psi\left(x, z\right), \tag{0.3}$$

where

- Ψ is the vector $\Psi^T(x,z) = (\psi_1(x,\, z), \psi_2(x,z))$, ^{T} being the symbol of transposition,

1991 *Mathematics Subject Classification.* 34E05, 34E20, 34L05.

Key words and phrases. almost periodic Schrödinger equation, singular spectrum, absolutely continuous spectrum, complex WKB method, monodromy matrix.

This paper was written while the authors were visiting the Mittag-Leffler Institute, Sweden. They are grateful for the support and hospitality.

- $M(z)$ is a 2×2 matrix with coefficients independent of x.

The matrix M is called *the monodromy matrix* associated to the consistent basis $(\psi_{1,2})$. More details and results on the monodromy matrix can be found in [11, 10].

For any consistent basis, the monodromy matrix satisfies

$$\det M(z) \equiv 1, \quad M(z+1) = M(z), \quad \forall z. \tag{0.4}$$

The above definition of the monodromy matrix applies to any 1-d quasi-periodic equation with two frequencies. It generalizes the definition of the monodromy matrix for one-dimensional periodic differential equations. As the potential in (0.1) is real, it is possible to construct a monodromy matrix of the form

$$M(z,E) = \begin{pmatrix} a(z,E) & b(z,E) \\ \overline{b(\overline{z},\overline{E})} & \overline{a(\overline{z},\overline{E})} \end{pmatrix} \tag{0.5}$$

0.1.1. *The monodromy equation.* Set $h = \dfrac{2\pi}{\varepsilon} \bmod 1$. Let M be a monodromy matrix associated to a consistent basis $(\psi_{1,2})$. Consider the *monodromy equation*

$$F_{n+1} = M(z+nh)F_n \qquad \forall n \in \mathbb{Z}. \tag{0.6}$$

We identify the vector solutions of (0.6) with functions $F : \mathbb{Z} \to \mathbb{C}^2$, we denote the values of F by F_n.

There are several deep relations between the monodromy equation and the family of equations (0.1). We describe only one of them. Let $2\pi/\varepsilon$ be irrational, and let $\Theta(E)$ (resp. $\theta(E)$) be the Lyapunov exponents for (0.1) (resp. for (0.6)). One proves

Theorem 0.1 ([11])**.** *The Lyapunov exponents $\Theta(E)$ and $\theta(E)$ satisfy the relation*

$$\Theta(E) = \frac{\varepsilon}{2\pi}\theta(E). \tag{0.7}$$

The passage to the monodromy equation is close to the monodromization idea developed in [3] for difference equations with periodic coefficients. For a detailed discussion, we refer to [11].

0.1.2. *The monodromy matrix in the adiabatic limit.* In the adiabatic limit i.e. when ε is small, using the complex WKB method developed in [9], one can compute the asymptotics of monodromy matrices. In all the cases we discuss in this review, we found the monodromy matrices to have the form

$$M(z,E) = M_0(E) + M_1(z,E) + R \tag{0.8}$$

- $M_0(E)$ is constant i.e. independent of z,
- $M_1(z,E)$ is a first order trigonometric polynomial in z,
- R is a smaller order remainder term.

The matrices M_0 and M_1 carry information on the location and the nature of the spectrum of (0.1). The asymptotic behavior of M_0 and M_1 depends on the spectral parameter. Essentially, there are four different types of asymptotic behavior for these matrices. So, the monodromy matrix (or the monodromy equation) gives a local (in energy) model describing the spectral properties of our initial differential equation (0.1).

0.2. **Some analytic objects related to periodic Schrödinger equations.** To formulate our results, we need to recall some information about the periodic Schrödinger operator

$$(H_0\psi)(x) = -\frac{d^2}{dx^2}\psi(x) + V(x)\psi(x) \tag{0.9}$$

acting in $L^2(\mathbb{R})$.

0.2.1. *The spectrum of H_0.* On $L^2(\mathbb{R})$, the spectrum of (0.9) is absolutely continuous and consists of *spectral bands* i.e. intervals $[E_1, E_2]$, $[E_3, E_4]$, ..., $[E_{2n+1}, E_{2n+2}]$, ..., of the real axis such that

$$E_1 < E_2 \le E_3 < E_4 \dots E_{2n} \le E_{2n+1} < E_{2n+2} \le \dots , \tag{0.10}$$

$$E_n \to +\infty, \quad n \to +\infty. \tag{0.11}$$

The open intervals (E_2, E_3), (E_4, E_5), ..., (E_{2n}, E_{2n+1}), ..., are called the *spectral gaps*. The ends of the bands are eigenvalues of the Schrödinger operator (0.9) with either periodic or anti-periodic boundary conditions at the ends of the interval $(0, 1)$. Some gaps can be closed (empty). In this case, connected components of the spectrum are unions of spectral bands with common ends. If $E_{2n} < E_{2n+1}$, we say that the n-th gap is open. From now on, we assume that

(O): all the gaps of the periodic operator are open.

0.2.2. *The Bloch quasi-momentum.* Let ψ be a solution of the periodic Schrödinger equation satisfying the relation $\psi(x+1) = \mu\,\psi(x), \ \forall x \in \mathbb{R}$, with μ independent of x. It is a *Bloch* solution, and μ is the *Floquet multiplier* associated to ψ. Write it as $\mu = \exp(ik)$; then, k is called the *Bloch quasi-momentum*. The Bloch solution ψ can be represented in the form $\psi(x) = e^{ikx}p(x)$ where $x \mapsto p(x)$ is a 1-periodic function.

The Bloch quasi-momentum is an analytic multi-valued function of E; it has branch points at the points E_1, E_2, E_3, ..., E_n, ...

Let D be a simply connected domain containing no branch points of the Bloch quasi-momentum. On D, fix k_0, an analytic single-valued branch of k. All the other single-valued branches that are analytic in $E \in D$, are described by the formulae

$$k_{\pm,l}(E) = \pm k_0(E) + 2\pi l, \quad l \in \mathbb{Z}. \tag{0.12}$$

Consider $\mathbb{C}_+$, the upper half of the complex plane. There exists k_p, an analytic branch of the complex momentum that conformally maps $\mathbb{C}_+$ onto the quadrant $\{\operatorname{Im} k > 0, \ \operatorname{Re} k > 0\}$ cut along finite vertical slits beginning at the points πl, $l = 1, 2, 3 \dots$ The branch k_p is continuous on $\mathbb{C}_+ \cup \mathbb{R}$. It is real and monotonically increasing along the spectrum; it maps the spectral band $[E_{2n-1}, E_{2n}]$ onto the interval $[\pi(n-1), \pi n]$. On the open gaps, $\operatorname{Im} k_p$ stays positive and has a single maximum that is non degenerate.

0.3. **The complex momentum.** The central analytic object of the complex WKB method is the *complex momentum* $\kappa(\zeta)$. It is defined in terms of the Bloch quasi-momentum of (0.9) by the formula

$$\kappa(\zeta) = k(E - W(\zeta)). \tag{0.13}$$

The complex momentum κ is a multi-valued analytic function. Its branch points are related to the branch points of the quasi-momentum by the relations

$$E_l = E - W(\zeta), \quad l = 1, 2, 3, \dots , \tag{0.14}$$

where $(E_l)_{l \ge 1}$ are the ends of the spectral gaps of the operator H_0. Each of these equations defines a periodic sequence of branch points.

Let D be a regular domain (i.e. a simply connected domain and containing no branch points of κ). Then, in D, one can fix κ_0, an analytic branch of κ. By (0.12), all the other analytic branches are described by the formulas

$$\kappa_m^{\pm} = \pm\kappa_0 + 2\pi m, \tag{0.15}$$

where $\pm$ and m are indexing the branches.

Consider the half-strip $\{\operatorname{Im}\zeta \ge 0, \ 0 \le \operatorname{Re}\zeta \le \pi\}$. On this strip, one defines the *main branch of the complex momentum* by

$$\kappa_p(\zeta) = k_p(E - W(\zeta)).$$

0.3.1. *The iso-energy curve.* Let $\mathbf{E}(\kappa)$ be the dispersion relation associated to H_0 that is the inverse of the the Bloch quasi-momentum k. Consider the *real* and the *complex iso-energy curves* $\Gamma_{\mathbb{R}}$ and Γ defined by

$$\Gamma_{\mathbb{R}}: \quad \mathbf{E}(\kappa) + W(\zeta) = E, \quad \kappa, \zeta \in \mathbb{R}, \tag{0.16}$$

$$\Gamma: \quad \mathbf{E}(\kappa) + W(\zeta) = E, \quad \kappa, \zeta \in \mathbb{C}. \tag{0.17}$$

The iso-energy curves $\Gamma_{\mathbb{R}}$ and Γ are 2π-periodic so in ζ as in κ. The curve $\Gamma_{\mathbb{R}}$ is symmetric with respect to the lines $\kappa = \pi l$, $l \in \mathbb{Z}$ and with respect to the lines $\zeta = \pi m$, $m \in \mathbb{Z}$.

The role of the real iso-energy curve for adiabatic problems is well known, see, for example [2]. Heuristically, the Hamiltonian $\mathbf{E}(\kappa) + W(\zeta)$ can be considered as an effective Hamiltonian for equation (0.1). Indeed, as the potential $W(\varepsilon x)$ oscillates very slowly, one can replace the periodic Schrödinger operator H_0 by its dispersion relation. This is analogous to the well known Peierls substitution.
Notice also that Γ, the complex iso-energy curve, is just the Riemann surface uniformizing κ.

0.4. **A general overview.** We begin with a very simple result on the asymptotic locus of the spectrum. Let $W_+ = \max_{x\in\mathbb{R}} W(x)$ and $W_- = \min_{x\in\mathbb{R}} W(x)$. Denote by $\Sigma(\varepsilon)$ the spectrum of (0.1) and by $\sigma(H_0)$ the spectrum of the periodic operator defined in (0.9). One has

Theorem 0.2 ([11])**.** *Let $\Sigma = \sigma(H_0) + W(\mathbb{R}) = \sigma(H_0) + [W_-, W_+]$. Then, one has*

- $\forall \varepsilon \geq 0$, $\Sigma(\varepsilon) \subset \Sigma$.
- *for any $K \subset \Sigma$ compact, there exists $\varepsilon_0 > 0$ and $C > 0$ such that, $\forall 0 < \varepsilon < \varepsilon_0$ and $\forall E \in K$, one has*

$$\Sigma(\varepsilon) \cap (E - C\sqrt{\varepsilon}, E + C\sqrt{\varepsilon}) \neq \emptyset.$$

We now present our results on the locus and on the nature of the spectrum of (0.1); we also discuss the transitions between the different spectral types. To do so, we slide the energy E along the spectral axis and study the various situation that occur. Let us discuss them very briefly. For an energy E, consider the "window" $\mathcal{W}(E) = [E - W_+, E - W_-]$. Theorem 0.2 already indicates that one of the crucial characteristic governing the spectrum at an energy E is the relative position of the interval $E - W(\mathbb{R})$ with respect to the spectrum of the operator H_0. One roughly has to distinguish between 4 different cases described in Fig. 1. Essentially, each case corresponds to a different topology

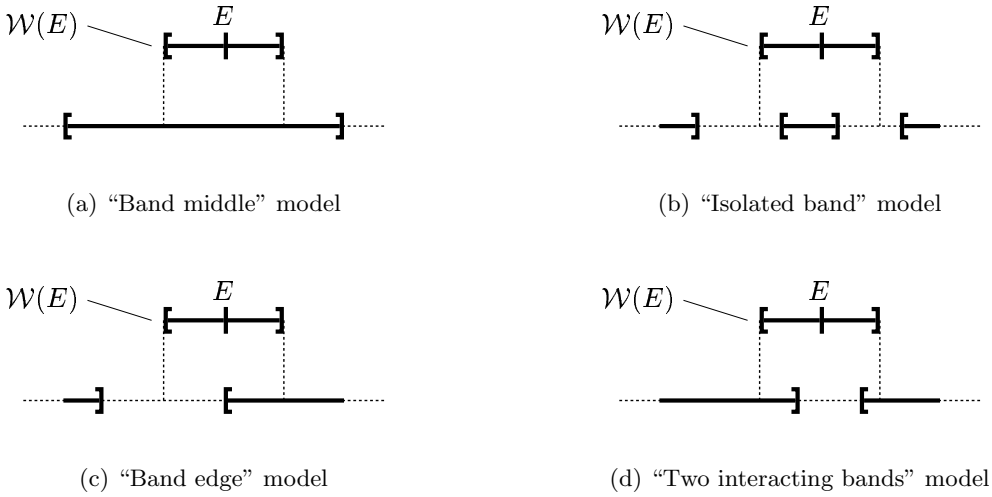

(a) "Band middle" model

(b) "Isolated band" model

(c) "Band edge" model

(d) "Two interacting bands" model

Figure 1: The four different cases

of the iso-energy curve Γ and to a different type of asymptotic behavior for the monodromy matrix.

1. The "band middle" model

We start with describing the energy regions for the "band middle" model (see Fig. 1(a)). Let $[E_{2n-1}, E_{2n}]$ be one of the spectral bands of the periodic operator H_0. We pick $J \subset \mathbb{R}$, a compact interval, such that

(BMM): $\mathcal{W}(E) \subset]E_{2n-1}, E_{2n}[$ for all $E \in J$.

Below, for the sake of definiteness, we assume that n is odd. In the case of even n, one gets similar results.

An interval J satisfying (BMM) exists if 2α, the "size" of the adiabatic perturbation, is smaller than the size of the spectral band $[E_{2n-1}, E_{2n}]$.

1.0.1. *The real iso-energy curve.* For the "band middle" model, the real iso-energy curve is described in Fig. 2(a). On this figure, the continuous curves are connected components of $\Gamma_{\mathbb{R}}$.

Under the condition (BMM), the main branch of the complex momentum, κ_p, maps the interval $[0, \pi]$ into $(\pi(n-1), \pi n)$. The graph of κ_p on this interval is a part of γ, a connected component of $\Gamma_{\mathbb{R}}$. Using the symmetry of $\Gamma_{\mathbb{R}}$ with respect to the line $\zeta = \pi$ and the its 2π-periodicity in ζ, we describe γ in Fig. 2(a). Using (0.15), one describes the other connected components of $\Gamma_{\mathbb{R}}$.

1.0.2. *Complex loops.* In Fig. 2(a), we show also dashed loops which are situated on Γ. To describe them, we turn to Fig. 2(b). This figure shows a few points from the periodic sequences of branch points of κ_p in the complex ζ-plane; these belong to the sequences of branch points closest to the real axis, i.e. defined by $E_l = E - W(\zeta_l)$ with $l = 2n-1$ and $l = 2n$. Along each of the loops $\tilde{\gamma}_0$ and $\tilde{\gamma}_\pi$, κ_p can be analytically continued to a single valued function. This observation implies that $\tilde{\gamma}_0$ and $\tilde{\gamma}_\pi$, are the projections of some loops in Γ; two of them, γ_0 and γ_π, are shown in Fig. 2(a).

1.0.3. *Action integrals and phases.* Let us now describe the actions and phases attached to the curves introduced above. We define *the phase integral* Φ attached to the curve γ by

$$\Phi(E) = \int_0^{2\pi} [\kappa_p(\zeta) - (n-1)\pi] d\zeta.$$

Under the condition (BMM), the function Φ is analytic in an neighborhood of J and it is positive for $E \in J$. Moreover, one checks that the derivative of Φ does not vanish on J. To the loops γ_0 and γ_π,

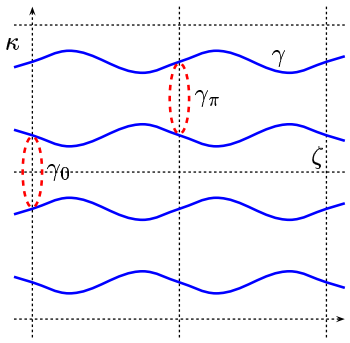

(a) The iso-energy curve

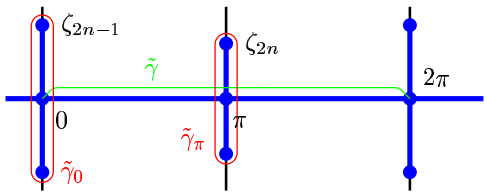

(b) The action and phase contours in the ζ-plane

Figure 2: The geometric objects in the "band middle" case

we attach the actions

$$S_{v,0}(E) = i \int_{\tilde{\gamma}_0} \kappa_p(\zeta) d\zeta, \quad S_{v,\pi}(E) = i \int_{\tilde{\gamma}_\pi} \kappa_p(\zeta) d\zeta.$$

On each loop, one can choose the orientation in such a way that the attached action be positive. These actions define a tunneling coefficient each

$$t_{v,0}(E) = \exp\left(-\frac{S_{v,0}(E)}{\varepsilon}\right) \text{ and } t_{v,\pi}(E) = \exp\left(-\frac{S_{v,\pi}(E)}{\varepsilon}\right) \tag{1.1}$$

1.1. **The spectral results.** Before formulating our precise spectral results, we describe a simple heuristics explaining them.

1.1.1. *The heuristics.* Consider the real iso-energy curve (0.16) depicted in Fig. 2(a). It consists of connected components stretching along the axis of ζ. In our case, the variable ζ plays the role of the coordinate in position space, while κ is the coordinate in momentum space. Standard semi-classical "wisdom" would say that the states of our system should live near the the iso-energy curve. At the view of Fig. 2(a), the states should extend in the position space. In Theorem 1.1, we prove that this is essentially the case. There are some energy intervals that are not covered by Theorem 1.1: this is due to possible tunneling in the vertical directions. The strength of this tunneling is measured by the tunneling coefficients $t_{v,0}$ and $t_{v,\pi}$. This tunneling can lead to the appearance of gaps in the spectrum.

1.1.2. *The spectral results.* We prove

Theorem 1.1 ([10])**.** *Let J be a nonempty closed interval satisfying the hypothesis (BMM). Fix $0 < \sigma < 1$. Then, there exists $D \subset (0,1)$, a set of Diophantine numbers such that*

- *one has*

$$\frac{\operatorname{mes}(D \cap (0,\varepsilon))}{\varepsilon} = 1 + o\left(\varepsilon\lambda^{\sigma}\right), \tag{1.2}$$

  where λ is defined by

$$\lambda = \exp\left(-\frac{S}{\varepsilon}\right), \quad \textit{and} \quad S = \min_{E\in J} \min\{S_{v,0}(E), S_{v,\pi}(E)\}.$$

- *for any $\varepsilon \in D$ sufficiently small, there exists a Borel set $B \subset J$ of small measure*

$$\frac{\operatorname{mes}(B)}{\operatorname{mes}(J)} = O(\lambda^{\sigma/2}),$$

  such that $J \setminus B$ belongs to the absolutely continuous spectrum of the equation family (0.1);
- *for all $E \in J \setminus B$, there exist two linearly independent Bloch-Floquet solutions $\psi_{\pm}(x,E)$ of (0.1) admitting the representations*

$$\psi_{\pm}(x) = e^{\pm ip(E)x}\, P_{\pm}(x - z, \varepsilon x, E), \tag{1.3}$$

  where $p(E)$ is a monotonously increasing, Lipschitz continuous function of E, the functions $P_{\pm}(x,\zeta,E)$ differ by the complex conjugation, $P_{-} = \overline{P_{+}}$, the function P_{+} is 1-periodic in x and 2π-periodic in ζ. This function belongs to H^2_{loc} in x and is analytic in ζ in a neighborhood of the real line. Moreover, P_{+} is a Lipschitz continuous function of E.

In Theorem 1.1, the coefficient λ is exponentially small in ε as $\varepsilon \to 0$. One can study the same problem for any real analytic periodic W (analyticity is essential for our method to work). In [10], we prove Theorem 1.1 in this greater generality but, in that case, we cannot give the optimal value of λ.

The Bloch-Floquet solutions $\psi_{\pm}$ described in Theorem 1.1 have the same functional structure as the Bloch-Floquet solutions constructed in [5, 6] for small almost periodic potentials or high energies. The regularity of the solutions $e^{\pm ip(E)x}\, P_{\pm}(x - z, \varepsilon x, E)$ in the "slow" variable εx is determined by the function W, and, in the "fast" variable $x - z$ by the function V.

1.2. **Asymptotics of a monodromy matrix.** To simplify the exposition, we formulate the results on the monodromy matrix in two Theorems. Assume the interval J satisfy assumption (BMM). We prove

Theorem 1.2 ([13]). *Let $E_0 \in J$. There exists $Y_0 > 0$ and V, a constant neighborhood of E_0, such that, for sufficiently small ε, the family of equations (0.1) has a consistent basis of solutions for which*

- *the corresponding monodromy matrix M is analytic in E in V and in z in the strip $\mathcal{S}_{Y_0} = \{|\operatorname{Im} z| \le Y_0/\varepsilon\}$,*
- *this matrix has the form (0.5).*

Now, we turn to the asymptotics of the monodromy matrix described in Theorem 1.2 for $\varepsilon \to 0$. We prove

Theorem 1.3 ([10]). *Fix $C_1,\ C_2 > 0$. Let $|E - E_0| \le C_1\varepsilon$ and $|\operatorname{Im}\zeta| \le C_2$. Then, for sufficiently small ε, the monodromy matrix defined in Theorem 1.2 has the following properties*

- *if we represent the coefficient a of the monodromy matrix as*

$$a = a_0 + \tilde{a}(z), \quad a_0 = \int_0^1 a(z)dz;$$

then, for $\varepsilon \to 0$, one has

$$a_0 = \exp(-i\Phi(E)/\varepsilon + o(1)), \quad \text{and} \quad \tilde{a} = O\left(e^{-\frac{S}{\varepsilon}}\right); \tag{1.4}$$

- *the coefficient b of the monodromy matrix admits the estimate*

$$b = O\left(e^{-\frac{S}{\varepsilon}}\right); \tag{1.5}$$

- *the estimates for a and b are uniform in (E, z).*

Theorem 1.3 is proved using the complex WKB method for adiabatic perturbations of periodic Schrödinger equations developed in [9].

Under our assumptions, one can actually compute the asymptotics of the coefficients $\tilde{a}$ and b. The leading term $\tilde{a}$ is given by $a_{-1}e^{-2i\pi z} + a_1 e^{2i\pi z}$, the sum of the first two terms of the Fourier series of a. The modulus of the Fourier coefficients are exponentially small in ε and can be expressed in terms $t_{v,0}$ and $t_{v,\pi}$.

1.3. **A very rough sketch of the proof of Theorem 1.1.** Let us explain how Theorem 1.3 is used to derive Theorem 1.1. By Theorem 1.3, the monodromy matrix is of the form

$$M = \begin{pmatrix} U & 0 \\ 0 & U^* \end{pmatrix} + O(\lambda),$$

where U is independent of z,

$$U = e^{-\frac{i}{\varepsilon}\Phi + o(1)}, \quad \lambda = e^{-\frac{S}{\varepsilon}}.$$

The relation $\det M \equiv 1$ implies that $|U| = 1 + o(\lambda)$ for $E \in J$. So, up to error terms of order $O(\lambda)$, M is a constant diagonal matrix with diagonal elements of absolute value 1. Now, consider the monodromy equation with the monodromy matrix M. If the error terms could be omitted, one would immediately obtain that, for all $E \in J$, there are bounded solutions of the monodromy equation. To take care of the exponentially small error terms, we apply standard ideas of the spectral KAM theory: we use a simple version (prepared in [11]) and construct bounded solutions of the monodromy equation for E outside of a Borel set B which is the countable union of intervals of small total measure. These intervals contain KAM resonances that can be roughly characterized by the "quantization condition"

$$\frac{1}{\pi\varepsilon}\Phi(E) = k \cdot h + l, \quad k, l \in \mathbb{Z}.$$

Having constructed bounded solutions of the monodromy equation outside of the set B, by Theorem 0.1, we conclude that the Lyapunov exponent of the equation family (0.1) is zero on $J \setminus B$. By

the Ishii-Pastur-Kotani Theorem [19], this implies that the essential closure of the set $J \setminus B$ belongs to the absolutely continuous spectrum of (0.1).

In Theorem 1.1, we have only described the part of the spectrum outside a small set. As said above, this set is related to the KAM resonances for the monodromy equation. We believe that, adapting the techniques developed in [6], one can prove that, in this small set, the spectrum is purely absolutely continuous.

2. The "isolated band" model

Let us describe the energy region corresponding to the "isolated band" model (see Fig. 1(b)). Actually, we consider a situation more general than the one depicted in Fig. 1(b): one is in the "isolated band" case when the spectral window $\mathcal{W}(E)$ completely covers at least one band i.e. it may cover totally or partially more than one band. For the sake of simplicity, we consider $J \subset \mathbb{R}$, a compact interval such that, for all $E \in J$, the window $\mathcal{W}(E)$ contains exactly $m+1$ isolated bands of the periodic operator. So, we fix two positive integers n and m and assume that

(IBM1): the bands $[E_{2(n+j)-1}, E_{2(n+j))}]$, $j = 0, 1, \dots m$, are isolated;
(IBM2): for all $E \in J$, these bands are contained in the interior of $\mathcal{W}(E)$;
(IBM3): for all $E \in J$, the rest of the spectrum of the periodic operator is outside of $\mathcal{W}(E)$.

Note that energies E satisfying (IBM1) – (IBM3) exist only if $W_+ - W_-$, the "size" of the adiabatic perturbation, is big enough; e.g., if $m = 0$, such energies exist if and only if $W_+ - W_-$ is larger than the size of the n-th spectral band, but smaller than the distance between the $(n-1)$-st and $(n+1)$-st bands.

2.1. Iso-energy curve.

We formulate our results in terms of the complex iso-energy curve (0.17). So, let us discuss it in detail.

2.1.1. *The real iso-energy curve.* Let us describe the real iso-energy curve (0.16) in the case of the IBM model. Consider the part of $\Gamma_{\mathbb{R}}$ in the strip $\{(\zeta, \kappa);\ 0 \le \zeta \le \pi\}$. The function $\zeta \mapsto E - W(\zeta)$ maps the interval $[0, \pi]$ onto $\mathcal{W}(E)$. Hence, by our assumptions (IBM1) – (IBM3), there are $m+1$ branch points of κ_p on the interval $(0, \pi)$; for $l = 2n-1, \dots, 2(n+m)$, the point ζ_l is defined by $E_l = E - W(\zeta_l)$. These points satisfy

$$0 < \zeta_{2n-1} < \zeta_{2n} < \dots < \zeta_{2(n+m)} < \pi.$$

The main branch of complex momentum, κ_p, is real on the intervals $\mathfrak{z}_j = [\zeta_{2j-1}, \zeta_{2j}]$, $j = n, n+1, \dots, n+m$. It takes complex values with positive imaginary part on the complement of these intervals in $[0, \pi]$. This implies that the part of $\Gamma_{\mathbb{R}}$ above the interval $[0, \pi]$ is located above the intervals $\mathfrak{z}_j$, $j = n, n+1, \dots, n+m$.

Fix $j = n, n+1, \dots, n+m$. On the interval $\mathfrak{z}_j$, κ_p is monotonously increasing from $(j-1)\pi$ to $j\pi$. This and (0.15) imply that, above $\mathfrak{z}_j$, the real iso-energy $\Gamma_{\mathbb{R}}$ consists of an continuous curve, 2π-periodic in the κ-direction.

To obtain the other connected components of $\Gamma_{\mathbb{R}}$, one just uses that it is symmetric with respect to the line $\zeta = \pi$ and 2π-periodic in the ζ-direction.

If $m = 0$ i.e.if the window $\mathcal{W}(E)$ contains only one isolated band, $\Gamma_{\mathbb{R}}$ is shown in Fig. 3(a). Here, we have drawn $\gamma_1^{\pm}$, two connected components of $\Gamma_{\mathbb{R}}$, projecting onto the intervals $\mathfrak{z}_n$ and $2\pi - \mathfrak{z}_n$. More details on its construction are given in [13].

2.1.2. *Complex loops.* Now, we discuss loops in the iso-energy curve (0.17) connecting connected components of $\Gamma_{\mathbb{R}}$.

Define the intervals

$$\begin{aligned} \mathfrak{g}_j^- = (\zeta_{2j}^-, \zeta_{2j+1}^-), \quad \mathfrak{g}_j^+ = (\zeta_{2j+1}^+, \zeta_{2j}^+), \quad j = n, n+1, \dots n+m-1, \\ \mathfrak{g}_{n-1} = (\zeta_{2n-1}^+ - 2\pi, \zeta_{2n-1}^-), \quad \mathfrak{g}_{n+m} = (\zeta_{2(n+m)}^-, \zeta_{2(n+m)}^+), \end{aligned} \tag{2.1}$$

and denote by $\mathcal{G}$ the set of these intervals.

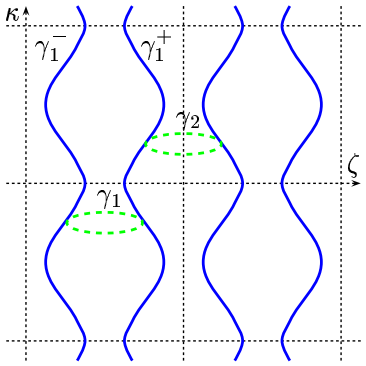

(a) The iso-energy curve

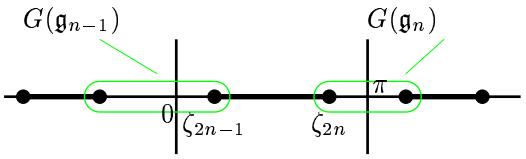

(b) The action and phase contours (when $m = 0$)

Figure 3: The geometric objects in the "isolated band" case

Let $\mathfrak{g} \in \mathcal{G}$, and let $V(\mathfrak{g}) \subset \mathbb{C}$ be a (complex) neighborhood of the interval $\mathfrak{g}$ containing only two branch points of the complex momentum, the ends of $\mathfrak{g}$. Let $G(\mathfrak{g})$ be a smooth closed curve that goes around the interval $\mathfrak{g}$ in $V(\mathfrak{g})$ intersecting the real axis twice. In Figure 3(b), we depicted the curves $G(\mathfrak{g})$ when $m = 0$.
In [13], we prove that, on each curve $G(\mathfrak{g})$, one can fix a continuous branch of the complex momentum. This implies that $G(\mathfrak{g})$ is the projection on $\mathbb{C}$ of a simple closed curve $\hat{G}(\mathfrak{g})$ situated on Γ; $\hat{G}(\mathfrak{g})$ connects the real branches of Γ situated above the intervals $\mathfrak{z} \in \mathcal{Z} \cup \{\mathfrak{z}^+_{2n-1} - 2\pi\}$ adjacent to $\mathfrak{g}$. For $m = 0$, in Fig. 3(a), we have shown loops γ_1 and γ_2 projecting onto $\hat{G}(\mathfrak{g}_\mathfrak{n})$ and $\hat{G}(\mathfrak{g}_{\mathfrak{n}-1}) + (2\pi, 0)$.

2.1.3. *Action integrals and phases.* To the real branches of the iso-energy curve, we associate the *phase integrals* defined by

$$\Phi(\mathfrak{z}) = \int_0^{2\pi} Z(\kappa, \mathfrak{z}) d\kappa, \quad \mathfrak{z} \in \mathcal{Z}. \tag{2.2}$$

All the phase integrals are real for $E \in J$ and analytic in E in a complex neighborhood of J.

To Γ, we associate the tunneling coefficients

$$t(\mathfrak{g}) = e^{-\frac{1}{2\varepsilon} S(\mathfrak{g})}, \quad \mathfrak{g} \in \mathcal{G}, \tag{2.3}$$

where $S(\mathfrak{g})$ are the actions given by

$$S(\mathfrak{g}) = i \oint_{G(\mathfrak{g})} \kappa(\zeta) d\zeta, \quad \mathfrak{g} \in \mathcal{G}. \tag{2.4}$$

In each of the integrals, we integrate a branch of the complex momentum continuous on the integration contour. We can and do choose the branches κ in (2.4) so that all the actions be positive for $E \in J$. Note that, with this choice, the tunneling coefficients become exponentially small as $\varepsilon \to 0$.

2.2. **Spectral results.** As in section 1.1, let us first describe the heuristics behind our spectral results.

2.2.1. *The heuristics.* In the present situation (see Fig. 3(a)), the real iso-energy curve is extended along the momentum axis. Hence, the quantum states should be extended in momentum and, thus, localized in the position space. Moreover, their possible extension along the position variable is governed by the tunneling between the vertical branches of $\Gamma_\mathbb{R}$ i.e. by the tunneling coefficients $t(\mathfrak{g})$. So, the Lyapunov exponent of equation (0.1) at energies in the "isolated band" zone should be related to this tunneling coefficient. This is the content of Theorem 2.1.

2.2.2. *The spectral results.* Our main spectral result is

Theorem 2.1 ([13]). *Let J be an interval satisfying the assumptions (IBM1)-(IBM3) for some n and m. Let W and V satisfy the hypothesis (H), and let $2\pi/\varepsilon$ be irrational. Then, on the interval J, for sufficiently small ε, the Lyapunov exponent $\Theta(E)$ for the family of equations (0.1) is positive and has the asymptotics*

$$\Theta(E) = \frac{\varepsilon}{2\pi}\sum_{\mathfrak{g}\in\mathcal{G}} \ln\frac{1}{t(\mathfrak{g})} + o(1) = \frac{1}{4\pi}\sum_{\mathfrak{g}\in\mathcal{G}} S(\mathfrak{g}) + o(1). \tag{2.5}$$

If $2\pi/\varepsilon$ is irrational, then $H_{z,\varepsilon}$ is quasi-periodic. In this case, its spectrum, its absolutely continuous spectrum and its singular spectrum do not depend on z (see [1, 18]); denote them respectively by Σ, Σ_{ac} and Σ_{s}. By the Ishii-Pastur-Kotani Theorem, see e.g [4, 19], Theorems 0.1, 0.2 and 2.1 imply

Corollary 2.1 ([13]). *In the case of Theorem 2.1, for ε sufficiently small, one has*

$$\Sigma(\varepsilon)\cap J \neq \emptyset \quad \text{and} \quad \Sigma_{ac}(\varepsilon)\cap J = \emptyset,$$

where $\Sigma_{ac}(\varepsilon)$ is the absolutely continuous spectrum of the family of equations (0.1).

2.3. **The asymptotics of the monodromy matrix.** As in the "band middle" case, Theorem 1.2 holds in this case too for J, an interval satisfying (IBM1) – (IBM3). Now, we turn to the asymptotics of the monodromy matrix described in Theorem 1.2 for the "isolated band" case. For the sake of definiteness, we assume n to be odd; in the case of even n, one obtains similar results. One has

Theorem 2.2. *In the case of Theorem 1.2, the coefficients a and b admit the asymptotic representations*

$$a = -iF_{-m}U^{-m}(z)(1+o(1)), \quad b = F_{-m}U^{-m}(z)(1+o(1)), \quad 0 < \operatorname{Im} z < Y_0/\varepsilon, \tag{2.6}$$

and

$$a = -iF_{m+1}U^{m+1}(z)(1+o(1)), \quad b = F_{m+1}U^{m+1}(z)(1+o(1)), \quad -Y_0/\varepsilon < \operatorname{Im} z < 0. \tag{2.7}$$

Here, F_{-m} and F_{m+1} are independent of z,

$$U(z) = e^{2\pi i z}, \quad F_{-m} = T^{-1}\exp\left(\frac{i}{2\varepsilon}\theta_0\right), \quad F_{m+1} = T^{-1}\exp\left(\frac{i}{2\varepsilon}\theta_1\right), \tag{2.8}$$

and

$$\begin{gathered} T = e^{-r}\textstyle\prod_{\mathfrak{g}\in\mathcal{G}} t(\mathfrak{g}), \quad \theta_0 = (\Phi(\mathfrak{z}_n^+) - \Phi(\mathfrak{z}_n^-)) + \textstyle\sum_{\mathfrak{g}\in\mathcal{G}\setminus\{\mathfrak{g}_n^\pm\}} \Phi(\mathfrak{g}) - 8\pi^2 m + 2\varepsilon s_0, \\ \theta_1 = -\textstyle\sum_{\mathfrak{g}\in\mathcal{G}} \Phi(\mathfrak{g}) + 8\pi^2(m+1) + 2\varepsilon s_1, \end{gathered} \tag{2.9}$$

where the functions r, s_0 and s_1 are independent of ε and real analytic in E in a neighborhood of E_0. The asymptotics for a and b are locally uniform in z and in E.

2.3.1. *The case of $m = 0$.* Theorem 2.2 does not describe the asymptotics of the coefficients a and b along the real axis of z. But, if $m = 0$, it implies

Theorem 2.3. *If, in the case of Theorem 1.2, $m = 0$, then the coefficients a and b admit the asymptotic representations*

$$a = -iF_0(1+o(1)) - iF_1U(z)(1+o(1)), \quad b = F_0(1+o(1)) + F_1U(z)(1+o(1)), \quad -Y_0/\varepsilon < \operatorname{Im} z < Y_0/\varepsilon. \tag{2.10}$$

These asymptotics are locally uniform in $E \in V$ and in z in the whole strip S_{Y_0}.

2.3.2. *A rough sketch of the proof of Theorem 2.1.* Let us now briefly explain how Theorem 2.1 is derived from the asymptotics of the monodromy matrix. For sake of simplicity, we assume that n is odd and $m = 0$. Up to error terms, the monodromy matrix then coincides with the matrix

$$M_0 = \begin{pmatrix} -i\mu(1+u) & \mu(1+u) \\ \mu^*(1+1/u) & i\mu^*(1+1/u) \end{pmatrix}, \qquad u = e^{2\pi i(z-\hat{z})}, \tag{2.11}$$
$$\hat{z} = \frac{1}{4\pi\varepsilon}(\theta_0(E) - \theta_1(E)), \quad \mu(E) = T^{-1}(E)e^{\frac{i}{2\varepsilon}\theta_0(E)}.$$

For the matrix M_0, one can calculate the Lyapunov exponent $\lim_{n\to\infty}\frac{1}{n}\ln\|M_0(z+nh)\dots M_0(z+h)M_0(z)\|$ explicitly. This and Theorem 0.1 lead to the formula (2.5). To justify this formula rigorously, we estimate the Lyapunov exponent for the cocycle generated by the monodromy matrix from below and from above. The upper bound follows directly from a simple norm estimate of (2.11). To get the lower bound, we use the ideas of [21] which generalize Herman's argument [16]. In result, we find that, up to a small error, the upper and the lower bounds coincide. Having calculated the Lyapunov exponent for the cocycle generated by the monodromy matrix, we use Theorem 0.1 and obtain (2.5).

Note that one can transform (in a standard way) the monodromy equation to a second order difference equation of the form

$$g(n+1) + \rho(nh+z)g(n-1) = v(nh+z)g(n), \quad n \in \mathbb{Z}, \tag{2.12}$$

for g taking values in $\mathbb{C}$. If $M(z)$ is analytic in z, then the coefficients $\rho(z)$ and $v(z)$ are meromorphic functions of z. Their poles are the zeros of the coefficient $M_{12}(z)$ of the monodromy matrix. For the monodromy matrix described in Theorem 2.3, these poles are situated in an exponentially small neighborhood of the real line; this is reminiscent of the Maryland model (see [4]).

3. The "band edge" model

The relative position of $\mathcal{W}(E)$ and the spectrum of H_0 is described in Fig. 1(c). More precisely, we consider a compact energy interval $J \subset \mathbb{R}$ such that, for all $E \in J$, the window $\mathcal{W}(E)$ contains exactly one edge, say E_{2n+1}, of a spectral zone of H_0, say $[E_{2n+1}, E_{2n+2}]$ i.e. we assume that there exists $\delta > 0$ such that, for all $E \in J$, one has

(BEM): $[E_{2n+1} - \delta, E_{2n+1} + \delta] \subset \mathcal{W}(E) \subset (E_{2n}, E_{2n+2})$.

For the sake of definiteness, we assume n is odd. The case of even n is dealt with in the same way. One can also consider the right hand side band edges. Mutandi mutandis, we obtain spectral results identical to those we describe now.

The results that we describe now extend those obtained for $n = 0$ in [11] i.e. at the bottom of the spectrum.

3.1. The geometric objects.

In the "band edge" case, the situation is more complicated than in the two previous cases, in the sense that there are more geometric objects (paths on Γ and phases and actions associated to them) that actually play a role both in the spectral analysis of equation (0.1) and in the description of the monodromy matrix. So, let us first start with describing these geometric objects.

3.2. The iso-energy curve.

Let us now describe the iso-energy curve Γ.

3.2.1. *The real iso-energy curve.* Consider the part of $\Gamma_{\mathbb{R}}$ above $\{(\zeta, \kappa);\ 0 \le \zeta \le \pi\}$. Under the hypothesis (H) and (BEM), the complex momentum κ has exactly one branch point, say ζ_{2n+1}, in the half-period $[0, \pi)$. The application $\mathcal{E} : \zeta \mapsto E - W(\zeta)$ maps the interval $[\zeta_{2n+1}, \pi]$ into the spectral band $[E_{2n+1}, E_{2n+2}]$, and it maps the interval $[0, \zeta_{2n+1})$ into the spectral gap (E_{2n}, E_{2n+1}). So, κ_p is real on $[\zeta_{2n+1}, \pi]$ and has positive imaginary part on $[0, \zeta_{2n+1})$. The graph of κ_p on the interval $[\zeta_{2n+1}, \pi]$ is a part (actually, one fourth) of γ_π, a connected component of $\Gamma_{\mathbb{R}}$. This connected component is diffeomorphic to a circle, and symmetric with respect to the lines $\zeta = \pi$ and $\kappa = (n-1)\pi$. All the other connected components of the real iso-energy curve can be obtained from γ_π by the 2π

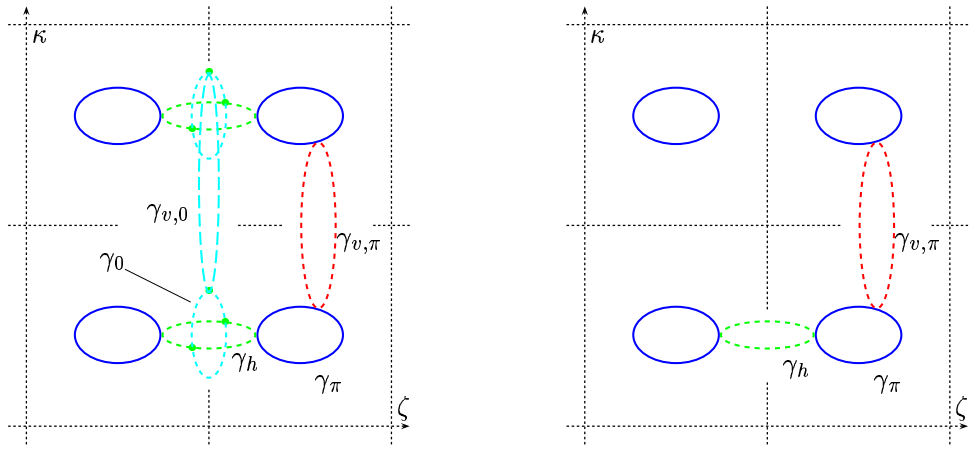

(a) In the general case

(b) When $n = 0$

Figure 4: The phase space picture

translations in the vertical and horizontal (i.e. κ- and ζ-) directions. In Fig. 4(a), we show an example of the real iso-energy curve.

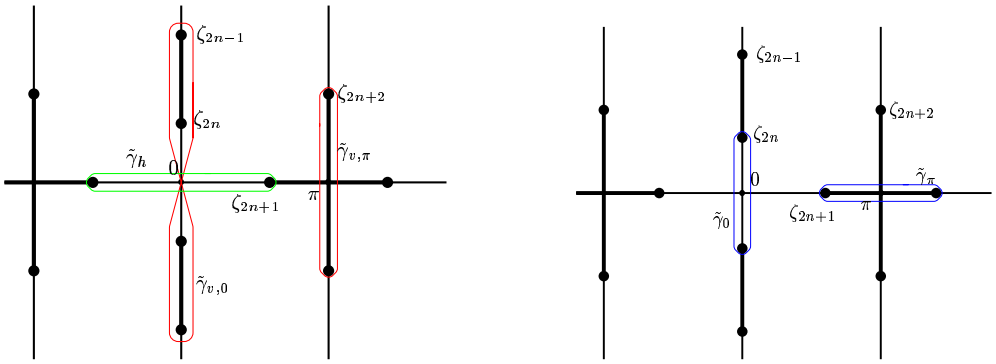

(a) The action contours

(b) The phase contours

Figure 5: The geometric objects in the "band edge" case

3.2.2. *Complex loops.* Let us now describe some useful complex loops in Γ. In Fig. 5, we have shown some branch points of the complex momentum. The points ζ_{2n-1}, ζ_{2n}, ..., ζ_{2n+2} are defined as in section 1.0.2.

First, we note that the complex momentum can be analytically continued along the contours $\tilde{\gamma}_0$, $\tilde{\gamma}_h$, $\tilde{\gamma}_{v,0}$ and $\tilde{\gamma}_{v,\pi}$ (see Fig. 5(a) and 5(b)). Hence, these loops are projection on the ζ-plane of loops, say γ_0, γ_h, $\gamma_{v,0}$ and $\gamma_{v,\pi}$, in Γ. In Fig. 4(a), we have tried to show these loops. The curve γ_h connects the real branches γ_π and $\gamma_\pi - (2\pi, 0)$. Here, $(\zeta, \kappa) + (2\pi, 0)$ denotes the 2π-translate of (ζ, κ) in the ζ-direction. The loop $\gamma_{v,\pi}$ connects the real branches γ_π and $\gamma_\pi + (0, 2\pi)$. The loop $\gamma_{v,0}$ connects the complex loops γ_0 and $\gamma_0 + (0, 2\pi)$. Moreover, as Fig. 6(a) shows, one can go from γ_π to $\gamma_\pi + (0, 2\pi)$ along the loops γ_h, γ_0, $\gamma_{v,0}$, $\gamma_0 + (0, 2\pi)$ and $\gamma_h + (0, 2\pi)$. None of the loops γ_h, γ_0, γ_π, $\gamma_{v,0}$ and $\gamma_{v,\pi}$ is contractible in Γ.

Let us now give an idea of the justification for the diagram 4(a). Therefore, consider the curve $\tilde{\gamma}_h$. Along the segment $[0, \zeta_{2n+1}]$ of this curve, one has

$$\operatorname{Re}\kappa_p(\zeta + i0) = n\pi,\ \operatorname{Im}\kappa_p(\zeta + i0) > 0 \quad \text{for} \quad 0 < \zeta < \zeta_{2n+1}, \quad \text{and} \quad \kappa_p(\zeta_{2n+1}) = \pi n.$$

Continuing κ_p analytically along the upper part of $\tilde{\gamma}_h$, we see that it satisfies

$$\kappa_p(-\zeta) = \kappa_p(\zeta)$$

as the cosine is even.
The upper half of $\tilde{\gamma}_h$ (see Fig. 5(a)) is the projection of the half of the curve γ_h described by

$$\{(\zeta, \kappa);\ \kappa = \kappa_p(\zeta + i0),\ \zeta \in [-\zeta_{2n+1}, \zeta_{2n+1}]\}.$$

Along the lower half of $\tilde{\gamma}_h$, one has

$$\kappa_p(\zeta - i0) = 2\pi n - \kappa(\zeta + i0),$$

and the second half of γ_h is

$$\{(\zeta, \kappa);\ \kappa = 2\pi n - \kappa_p(\zeta + i0),\ \zeta \in [-\zeta_{2n+1}, \zeta_{2n+1}]\}.$$

Finally, note that, for γ, a given loop in Γ, its 2π-translates in the ζ- or in the κ-directions are also loops in Γ. Moreover, if γ projects on $\tilde{\gamma}$ in the ζ-plane, so do its 2π-translates in the κ-direction.

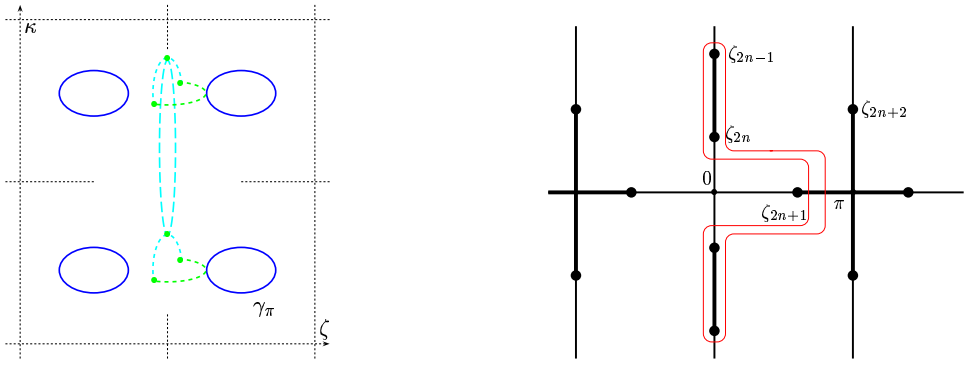

(a) (b)

Figure 6:

3.2.3. *The phases integrals.* Pick $\alpha \in \{0, \pi\}$. To $\tilde{\gamma}_\alpha$ (or equivalently γ_α), we associate the *phase integral* Φ_α defined by

$$\Phi_\alpha(E) = \frac{1}{2}\oint_{\gamma_\alpha} \kappa(\zeta)\, d\zeta = \frac{1}{2}\oint_{\tilde{\gamma}_\alpha} \kappa_p(\zeta)\, d\zeta.$$

The phase integral Φ_α is real analytic and monotonous in $E \in J$. The direction of the integration is chosen so that $\Phi_\alpha(E)$ be positive. Then, $\Phi'_\alpha(E) > 0$.

3.2.4. *The action integrals and the tunneling coefficients.* We define the horizontal action integral S_h by

$$S_h(E) = -\frac{i}{2}\oint_{\gamma_h} \kappa(\zeta)\, d\zeta.$$

For $E \in J$, this integral is real analytic. By definition, we choose the direction of integration so that $S_h(E)$ be positive. The tunneling coefficient in the horizontal direction is the function

$$t_h(E) = \exp\left(-\frac{1}{\varepsilon}S_h(E)\right).$$

Pick $\alpha \in \{0, \pi\}$. To the loop $\gamma_{v,\alpha}$, we associate the action $S_{v,\alpha}$ defined by

$$S_{v,\alpha}(E) = -\frac{i}{2} \oint_{\gamma_{v,\alpha}} \kappa d\zeta,$$

and the tunneling coefficient

$$t_{v,\alpha}(E) = \exp\left(-\frac{1}{\varepsilon} S_{v,\alpha}(E)\right).$$

For $E \in J$, the action $S_{v,\alpha}(E)$ is real analytic. By definition, we chose the direction of integration so that $S_{v,\alpha} > 0$.

As we have seen, in Γ, there are two paths, the loop $\gamma_{v,\pi}$ and the path shown in Fig. 6(a), that connect γ_π and its 2π-translate in the κ-direction. There are many more such paths. To each such path, one can associate an action in the same way as above. The smallest possible action obtained in that way is either $S_{v,\pi}$ or $S_{v,0}$ i.e. the one attached to $\gamma_{v,\pi}$ or to the path shown in Fig. 6(a). To guarantee that these are actually the two paths with smallest actions, we assume that

(P): for $k \leq 2n-2$ and $k \geq 2n+3$, $\operatorname{Im} \zeta_k > \max(\zeta_{2n-1}, \zeta_{2n+2})$.

This condition can be relaxed quite a lot as the true condition has to be written in term of the actions.

To complete this section, let us note that, when one deals with the case $n = 0$ (i.e. the lowest band edge, that is, the bottom of the spectrum), the loops γ_0 and $\gamma_{v,0}$ do not exist. Fig. 4(a) is replaced with Fig. 4(b). Note also that, in this case, the action $S_{v,\pi}$ attached to $\gamma_{v,\pi}$ is always the smallest one.

3.3. **The spectral results.** Assume that the assumptions (H), (O), (BEM) and (P) are satisfied.

3.3.1. *The heuristics.* In the "band edge model" case, the iso-energy curve is more complicated than in the two previous situation. Now, $\Gamma_{\mathbb{R}}$ is a periodic array of loops (γ_π and its 2π-translates in the κ- and ζ- directions); topologically, each loop is a one-dimensional tori.

Semi-classically, each of these tori carries states given by a Bohr-Sommerfeld like quantization condition (described by the phase integral Φ_π introduced in section 3.2.3). So,the spectrum should be located near the energies defined by these quantization conditions. This is the content of Theorem 3.1. The states then interact through tunneling between the various tori. The tunneling is governed by the coefficients t_h, $t_{v,0}$ and $t_{v,\pi}$. One can expect that if it is easier to tunnel in the horizontal (resp. vertical) direction (i.e. if the horizontal (resp. vertical) tunneling coefficient t_h (resp. $t_{v,0}$ or $t_{0,\pi}$) is larger), the particle will extend in the horizontal (resp. vertical) direction. So, if tunneling is stronger in the vertical direction, one expects singular spectrum with a positive Lyapunov exponent, this one being controlled by the tunneling coefficients; this is the content of Theorem 3.2. At energies where the tunneling is stronger in the horizontal direction, one expects states to be extended in the position variable i.e. to give rise to absolutely continuous spectrum; this is the content of Theorem 3.3.

As underlined in section 3.2.4, under the hypothesis (P), $t_{v,0}$ and $t_{0,\pi}$ are the smallest of the coefficients responsible for the tunneling in the vertical direction. It is natural to wonder which one governs the localization-delocalization phenomenon. One could expect it to be the smallest one. In general, this is not so. The tunneling coefficient $t_{v,\pi}$ attached to the loop $\gamma_{v,\pi}$ connecting the tori of $\Gamma_{\mathbb{R}}$, i.e. the tori giving the quantization condition, plays a special role; it is this tunneling coefficient that governs the nature of the spectrum and the spectral transitions (see section 3.4).

3.3.2. *The spectral results.* We first state a result on the location of the spectrum in J. Therefore, we recall that the function $\Phi_\pi(E)$ is monotonically increasing on J and that its derivative does not vanish there. Moreover, $\Phi_\pi(E) > 0$. There is a real analytic function $\check{\Phi}_\pi(E)$ defined in a neighborhood of J and having the uniform asymptotics

$$\check{\Phi}_\pi(E) = \Phi_\pi(E) + o(\varepsilon). \tag{3.1}$$

This function is the phase defining the quantization conditions. In J, consider the points $E^{(l)}$, $l \in \mathbb{N}$, defined by

$$\frac{1}{\varepsilon}\check{\Phi}_\pi(E^{(l)}) = \frac{\pi}{2} + \pi l, \quad l \in \mathbb{N}.$$

The number of these points is finite; we denote the minimal and the maximal values of l by L_1 and L_2. For sufficiently small ε, the distances between these points satisfy the inequalities

$$c_1\varepsilon \leq E^{(l)} - E^{(l-1)} \leq c_2\varepsilon, \quad l = L_1 + 1, \ldots, L_2$$

where c_1 and c_2 are two positive constants independent of ε. We then prove

Theorem 3.1. *For $\varepsilon > 0$ sufficiently small, there exists a collection of intervals $(I_l)_{L_1 \leq l \leq L_2}$, $I_l \subset J$, such that one has*

- $\Sigma \cap J \subset \cup_{L_1 \leq l \leq L_2} I_l$,
- *the interval I_l contains $E^{(l)}$,*
- *the measure of I_l is estimated by*

$$|I_l| \leq C\frac{\varepsilon(t_{v,\pi}(E^{(l)}) + t_h(E^{(l)}))}{\Phi'_\pi(E^{(l)})}(1 + o(1)).$$

Moreover, if $dN_\varepsilon(E)$ denotes the density of states measure of $H_{z,\varepsilon}$ at energy E, then, one has

$$\int_{I_l} dN_\varepsilon(E) = \frac{1}{2\pi}\varepsilon. \tag{3.2}$$

Note that the intervals I_l are exponentially small and separated by a distance of order $O(\varepsilon)$.

Now, let us discuss the nature of the spectrum. Set

$$\lambda(E) = t_{v,\pi}(E)/t_h(E), \quad \Delta S(E) = \varepsilon \log \lambda(E) = (S_h(E) - S_{v,\pi}(E)).$$

For $\delta \geq 0$, define the set

$$J_\delta^- = \{E \in J;\ \Delta S(E) < -\delta\}$$

If $J_\delta^- \neq \emptyset$, then, for sufficiently small ε, the number of intervals I_l lying in J_δ^- is of order $O(1/\varepsilon)$. Finally, let $\tilde{\lambda}(E) = \lambda(E) + t_{v,0}(E)$. We prove

Theorem 3.2. *Fix $C > 0$ large. Pick $E_0 \in J$ and let V_0 be the $C\varepsilon$-neighborhood of E_0 in J. Pick $\sigma \in (0,1)$. Then, there exists $D \subset (0,1)$ a set of Diophantine numbers such that*

- $$\frac{\operatorname{mes}(D \cap (0,\varepsilon))}{\varepsilon} = 1 + o\left(\varepsilon^2\tilde{\lambda}^\sigma\right) \text{ when } \varepsilon \to 0, \quad \tilde{\lambda} = \tilde{\lambda}(E_0).$$
- *For any ε small enough and $\varepsilon \in D$, each of the intervals $I_l \subset V_0$ contains absolutely continuous spectrum, and, for these intervals,*

$$\frac{\operatorname{mes}(I_l \cap \Sigma_{\mathrm{ac}})}{\operatorname{mes} I_l} = 1 + O(\tilde{\lambda}^{\sigma/2}), \quad \tilde{\lambda} = \tilde{\lambda}(E_0).$$

Here, Σ_{ac} is the absolutely continuous spectrum of $H_{z,\varepsilon}$.

Fix δ positive and let

$$J_\delta^+ = \{E \in J;\ \Delta S(E) > \delta\}.$$

As before, if $J_\delta^+ \neq \emptyset$, then, for sufficiently small ε, the number of intervals I_l lying in J_δ^+ is of order $O(1/\varepsilon)$. We prove

Theorem 3.3. *For sufficiently small ε, each of the intervals $I_l \subset J_\delta^+$ contains only singular spectrum; moreover, in the interval I_l, one has*

$$\Theta(E) = \frac{\varepsilon}{2\pi}\log\lambda(E^{(l)}) + o(1) = \frac{1}{2\pi}\left(S_h(E^{(l)}) - S_{v,\pi}(E^{(l)})\right) + o(1).$$

3.4. **The asymptotics of the monodromy matrix.** Again, Theorem 1.2 holds for J, a compact energy interval satisfying (BEM). Under the hypothesis (BEM) and (P), the monodromy matrix admits the representation (0.8). Each of the matrices in this representation is of the form (0.5). The coefficients of M_0 have the asymptotics

$$a_0 = a_0(E) = \frac{1}{t_h(E)}\, e^{i\Phi_\pi(E)/\varepsilon}(1+o(1)), \quad b_0 = b_0(E) = \frac{i}{t_h(E)}\, e^{i\Phi_\pi(E)/\varepsilon}(1+o(1)), \tag{3.3}$$

and the Fourier coefficients of the matrix M_1 are bounded by $\max\left\{\frac{t_{v,0}(E)}{t_h(E)},\ \frac{t_{v,\pi}(E)}{t_h(E)}\right\}$.

Our analysis of the monodromy equation (0.6) reveals that, under our assumptions, the two important characteristics of the monodromy matrix are the trace of the zeroth and first Fourier coefficients of M; we denote them by $[\operatorname{tr}(M)]_{0,1}$ and define

$$F(E) = [\operatorname{tr}(M)]_0 \quad \text{and} \quad \lambda(E) = |[\operatorname{tr}(M)]_1|$$

We call the function $F(E)$ the *effective spectral parameter*, and $\lambda(E)$ is the *effective coupling constant*. These two objects then characterize the spectrum in the following way:

- energies E satisfying $|F(E)| > C(\lambda(E)+1)$ are in the resolvent set of $H_{z,\varepsilon}$ (for some fixed $C>0$); actually, for such energies, one can construct two linearly independent solutions to equation (0.1) such that one is exponentially decreasing at $+\infty$ and the other is exponentially decreasing at $-\infty$;
- for the energies E such that $|F(E)| \le C(\lambda(E)+1)$, the Lyapunov exponent of $H_{z,\varepsilon}$ is given by

$$\Theta(E) = \frac{1}{2\pi}\cdot\max(0, \varepsilon\cdot\log\lambda(E) + o(1)).$$

Using the asymptotics of the monodromy matrix, one proves that

$$F(E) = 2e^{S_h(E)/\varepsilon}\left(\cos\left(\frac{\Phi_\pi}{\varepsilon}\right) + o(1)\right) \tag{3.4}$$

and

$$\lambda(E) = \left|\nu\, e^{(S_h(E)-S_{v,\pi}(E))/\varepsilon}\,(1+o(1)) + e^{(S_h(E)-S_{v,0}(E))/\varepsilon}\left(\cos\left(\frac{\Phi_\pi}{\varepsilon}\right)+o(1)\right)\right| \tag{3.5}$$

Here, $\nu = \exp(-2i\pi^2/\varepsilon)$.

One of the crucial points in our analysis is that, under assumption (P), the factors $\cos\left(\frac{\Phi_\pi}{\varepsilon}\right)+o(1)$ in the formulas for $F(E)$ and in that for $\lambda(E)$ are proportional to each other, up to an exponentially small error. Actually, one proves that, if $\operatorname{Re}E \in J$, $|\operatorname{Im}E| \le C_1$, where C_1 is a fixed positive constant, then

$$\begin{aligned}\operatorname{Tr}M(z) = {} & 2e^{\frac{S_h(E)}{\varepsilon}+o(1)}\,\cos\left(\frac{\check\Phi_\pi}{\varepsilon}\right) + O(1)\\ & + 2\left|e^{\frac{S_h(E)-S_{v,\pi}(E)}{\varepsilon}+o(1)} + \nu\, e^{\frac{S_h(E)-S_{v,0}(E)}{\varepsilon}+o(1)}\,\cos\left(\frac{\check\Phi_\pi}{\varepsilon}\right)\right|\cos(2\pi(z-z_0(E)))\\ & + O\left(\max_\alpha\{t_{v,\alpha}\} + e^{-C/\varepsilon}\,\frac{\min_\alpha(t_{v,\alpha})}{t_h} + \frac{t_{v,0}t_{v,\pi}}{t_h}\right),\end{aligned} \tag{3.6}$$

where $o(1)$ and $O(1)$ are independent of z, C is a positive constant and $z_0(E)$ is a real analytic function. This explains why the nature of the spectrum is defined by $t_{v,\pi}$ and not by $t_{v,0}$.

Remark 3.1. The proof of (3.6) is based on a factorization of the monodromy matrix in a product of two matrices:

$$M(z) = Q^{-1}(z)\cdot P(z) \text{ where } P(z) = \begin{pmatrix}\alpha & \beta\\ \beta^* & \alpha^*\end{pmatrix} \text{ and } Q(z) = \begin{pmatrix}\gamma & \delta\\ \delta^* & \gamma^*\end{pmatrix}. \tag{3.7}$$

The matrices P and Q are 1-periodic in z, and, which plays a very important role, their determinants are independent of z. This factorization comes about very naturally in our method of computation of the monodromy

matrix: there are two natural consistent bases and each of the factors is a transfer matrix between these consistent bases.

For $j \in \mathbb{Z}$, let α_j (resp. β_j, γ_j, δ_j), denote the j-th Fourier coefficient of α (resp. β, γ, δ). Under the assumptions (H), (O), and (BEM), one has

$$\alpha = \alpha_0(1+o(1)) + \alpha_1 u(1+o(1)), \quad \beta = \beta_0(1+o(1)) + \beta_1 u(1+o(1)),$$

$$\gamma = \gamma_0(1+o(1)) + \gamma_{-1}u^{-1}(1+o(1)), \quad \delta = \delta_0(1+o(1)) + \delta_1 u(1+o(1)), \tag{3.8}$$

$$u = e^{2i\pi z}.$$

Actually, in these asymptotics , the terms $o(1)$ are exponentially small in ε.
The Fourier coefficients are given by

$$\alpha_0 = \frac{1}{\sqrt{t_h}} e^{i\frac{\Phi_\pi}{2\varepsilon} + A_0 + o(1)}, \quad \beta_0 = \frac{1}{\sqrt{t_h}} e^{-i\frac{\Phi_\pi}{2\varepsilon} + B_0 + o(1)},$$
$$\gamma_0 = \frac{1}{\sqrt{t_h}} e^{i\frac{\Phi_0}{\varepsilon} - i\frac{\Phi_\pi}{2\varepsilon} + C_0 + o(1)}, \quad \delta_0 = \frac{1}{\sqrt{t_h}} e^{i\frac{\Phi_0}{\varepsilon} + i\frac{\Phi_\pi}{2\varepsilon} + D_0 + o(1)},$$
$$\alpha_1 = \alpha_0 \cdot (G_0 + o(1)) \cdot t_{v,0} e^{A_1 + o(1)}, \quad \beta_1 = \beta_0 \cdot (G_0 + o(1)) \cdot t_{v,0} e^{B_1 + o(1)},$$
$$\gamma_{-1} = \gamma_0 t_{v,\pi} e^{i\frac{\Phi_\pi}{\varepsilon} - \frac{2i\pi^2}{\varepsilon} + C_1 + o(1)}, \quad \delta_1 = \delta_0 t_{v,\pi} e^{-i\frac{\Phi_\pi}{\varepsilon} + \frac{2i\pi^2}{\varepsilon} + D_1 + o(1)},$$

where $A_{0,1}$, $B_{0,1}$, $C_{0,1}$,$D_{0,1}$ are constants, independent of ε and E.

Note also that the determinants of P and Q coincide, and admit the representation

$$\mathrm{Det}\, P = \mathrm{Det}\, Q = C(E) \cdot (G_0 + o(1)), \quad \text{where} \quad G_0(E) = \cos\left(\frac{\Phi_0}{\varepsilon}\right). \tag{3.9}$$

Here, the coefficient C is independent of ε and does not vanish, and the factor $G_0 + o(1)$ vanishes on a discrete set of points $E \in \mathbb{R}$. The latter, however, does not play a too important role as one knows that M is analytic in E.

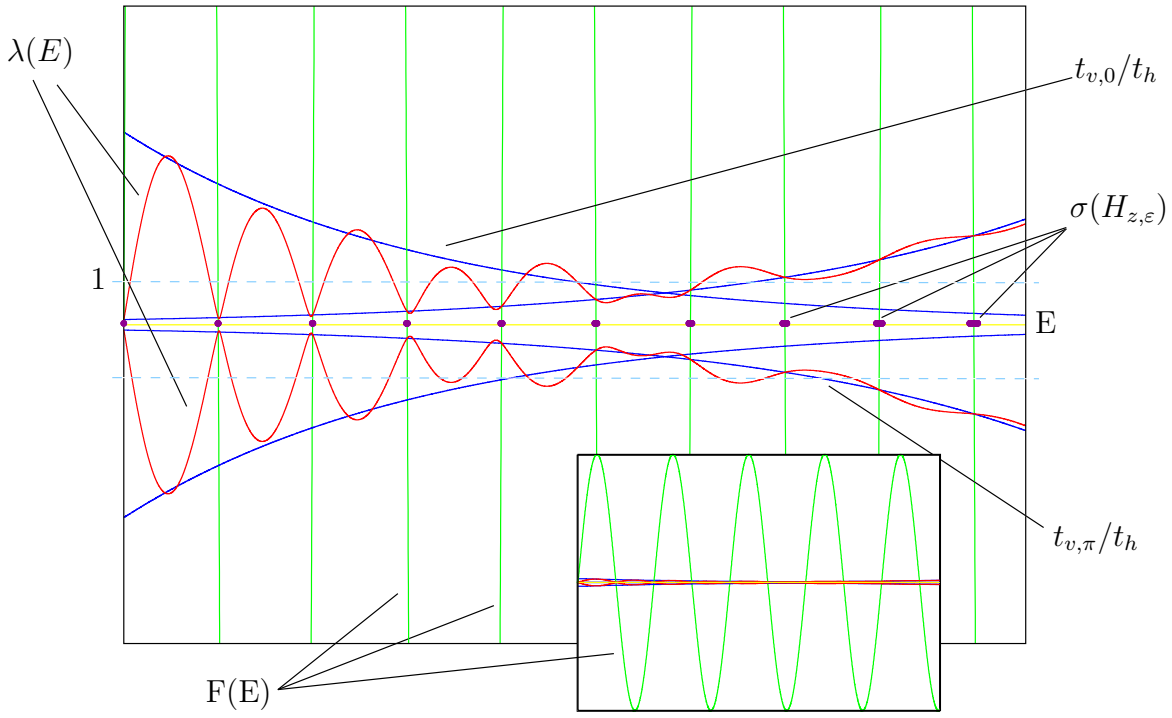

Figure 7: Analysis of the traces of monodromy matrix in the "band edge" case

The spectral results described in section 3.3 can then be summed up in a picture similar to the one obtained when studying the Lyapunov function (i.e. the trace of the monodromy matrix) for periodic one-dimensional Schrödinger operators. An example of such a picture is shown in Fig. 7. We represented the energy axis horizontally, and the coupling constant λ, the ratios of the tunneling coefficients and the effective spectral parameter F vertically. The effective spectral parameter $F(E)$ oscillates at a high frequency (roughly $1/\varepsilon$) and with a large amplitude (roughly $1/t_h$). The graph of λ is oscillating between the graphs of the ratios $t_{v,0}/t_h$ and $t_{v,\pi}/t_h$. The spectrum is contained in the intervals defined by $|F(E)| \leq C(\lambda(E)+1)$, and in each of the intervals, the nature of the spectrum is obtained by comparing the graph of λ and the graph of $|y| = 1$ (depicted by the dashed curve). Roughly, when $|\lambda| < 1$, the spectrum is absolutely continuous, when $|\lambda| > 1$, it is singular.

4. The "two interacting bands" model

In this last section, we assume that the compact energy interval J is chosen so that, there exists $\delta > 0$ such that, for all $E \in J$, one has

(TIBM): $(E_{2n} - \delta, E_{2n+1} + \delta) \subset \mathcal{W}(E) \subset]E_{2n-1}, E_{2n+2}[$, for all $E \in J$.

4.1. **The geometric objects.** In the "two interacting bands" case, the situation is close to the one in the "band edge" case. We will use this fact when describing the geometric objects.

4.2. **The iso-energy curve.** Let us now describe the iso-energy curve Γ.

Consider the part of $\Gamma_{\mathbb{R}}$ above $\{(\zeta, \kappa);\ 0 \leq \zeta \leq \pi\}$. Under the hypothesis (H) and (TIBM), the complex momentum κ has exactly two branch points, say ζ_{2n} and ζ_{2n+1}, in the half-period $[0, \pi)$. The application $\mathcal{E} :\ \zeta \mapsto E - W(\zeta)$ maps the interval $[\zeta_{2n+1}, \pi]$ into the spectral band $[E_{2n+1}, E_{2n+2}]$, the interval $[0, \zeta_{2n}]$ into the spectral band $[E_{2n-1}, E_{2n}]$, and it maps the interval $(\zeta_{2n}, \zeta_{2n+1})$ onto the spectral gap (E_{2n}, E_{2n+1}). So, κ_p is real on $[\zeta_{2n+1}, \pi]$ and $[0, \zeta_{2n}]$, and it has positive imaginary part on $[\zeta_{2n}, \zeta_{2n+1})$. On each of the intervals $[0, \zeta_{2n}]$ and $[\zeta_{2n+1}, \pi]$, the graph of κ_p is a part of a connected component of $\Gamma_{\mathbb{R}}$. These two connected components are disjoint and diffeomorphic to circles. Moreover, the one corresponding to $[\zeta_{2n+1}, \pi]$, say γ_π, is symmetric with respect to the line $\zeta = \pi$ and, the one corresponding to $[0, \zeta_{2n}]$, say γ_0, is symmetric with respect to the line $\zeta = 0$. Both are symmetric with respect to the line $\kappa = (n-1)\pi$. All the other connected components of the real iso-energy curve can be obtained from γ_0 and γ_π by the 2π translations in the vertical and horizontal (i.e. κ- and ζ-) directions. In Fig. 8, we show an example of the real iso-energy curve.

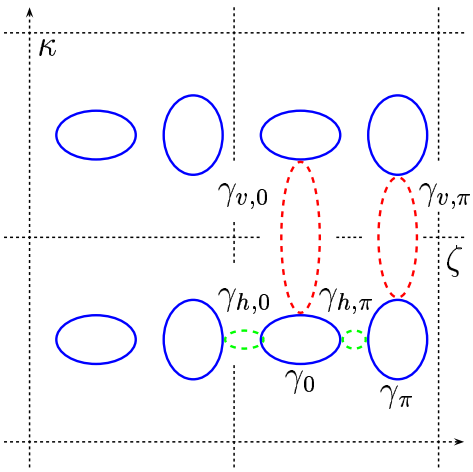

Figure 8: The phase space picture

So, we see that, now, each periodicity cell contains two distinct connected components of $\Gamma_{\mathbb{R}}$. Compare it with $\Gamma_{\mathbb{R}}$ from the "band edge" case. The connected components γ_0 and γ_π in the "two interacting bands" case are obtained from their homonyms in the "band edge" case by homotopy (the parameter being the spectral parameter E); the loop γ_0 that was complex now becomes real (compare Fig. 4(a) with Fig. 8).

4.2.2. *Complex loops.* Now, the configuration of the branch points of the complex momentum is given in Fig. 9. The points ζ_{2n-1}, ζ_{2n}, ..., ζ_{2n+2} are defined as before.

The complex momentum can be analytically continued along the contours $\tilde{\gamma}_0$, $\tilde{\gamma}_{h,0}$, $\tilde{\gamma}_{h,\pi}$, $\tilde{\gamma}_{v,0}$ and $\tilde{\gamma}_{v,\pi}$ (see Fig. 9(a) and 9(b)). Hence, these loops are projection on the ζ-plane of loops, say γ_0, $\gamma_{h,0}$, $\gamma_{h,\pi}$, $\gamma_{v,0}$ and $\gamma_{v,\pi}$, in Γ. In Fig. 8, we have tried to show these loops. The loop $\gamma_{h,\pi}$ connects the real

branches γ_π and γ_0; the loop $\gamma_{h,0}$ connects the real branches γ_0 and $\gamma_\pi - (2\pi, 0)$. The loop $\gamma_{v,\pi}$ connects the real branches γ_π and $\gamma_\pi + (0, 2\pi)$; the loop $\gamma_{v,0}$ connects the real branches γ_0 and $\gamma_0 + (0, 2\pi)$.

Note that the loop γ_h found in the "band edge" case has, in the "two interacting bands" case, split into two loops $\gamma_{h,0}$ and $\gamma_{h,\pi}$.

4.2.3. *The phase integrals, the action integrals and the tunneling coefficients.* Pick $\alpha \in \{0, \pi\}$. To $\tilde{\gamma}_\alpha$ (or equivalently γ_α), we associate the *phase integrals* Φ_α defined as in section 3.2.3; to the loops $\gamma_{v,\alpha}$, we associate the actions $S_{v,\alpha}$ defined as in section 3.2.4. The main properties of these phase integrals and actions remain the same as in the "band edge" case.

Let us notice here that the phases Φ_0 and Φ_π and the action $S_{v,\pi}$ are obtained by analytic continuation in E from their homonyms in the "band edge" case. The situation for $S_{v,0}$ and S_h is more complicated.

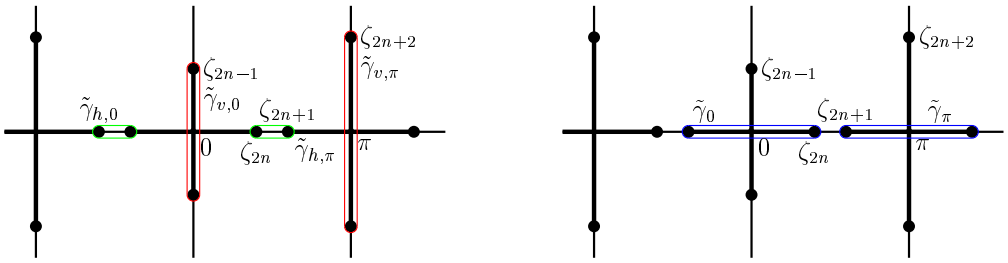

(a) The action contours

(b) The phase contours

Figure 9: The geometric objects in the "two interacting bands" case

For α as above, we define the horizontal action integrals $S_{h,\alpha}$ by

$$S_{h,\alpha}(E) = -\frac{i}{2} \oint_{\gamma_{h,\alpha}} \kappa(\zeta)\, d\zeta.$$

For $E \in J$, these integrals are real. By definition, we choose the direction of integration so that $S_{h,\alpha}(E)$ be positive. The tunneling coefficients in the horizontal direction are the functions

$$t_{h,\alpha}(E) = \exp\left(-\frac{1}{\varepsilon} S_{h,\alpha}(E)\right).$$

We note that we now have two horizontal tunneling coefficients $t_{h,0}$ and $t_{h,\pi}$. The parity of the cosine implies that

$$S_{h,0}(E) = S_{h,\pi}(E) \text{ and } t_{h,0}(E) = t_{h,\pi}(E).$$

Remark 4.1. In the present review, we have restricted ourselves to $W(x) = \alpha \cos(x)$. For general W, i.e. when W is not even, the actions $S_{h,\pi}$ and $S_{h,0}$, and the tunneling coefficients $t_{h,\pi}$ and $t_{h,0}$ need not to be equal.

We define

$$S_h(E) = S_{h,0}(E) + S_{h,\pi}(E) \quad \text{and} \quad t_h(E) = t_{h,0}(E) \cdot t_{h,\pi}(E). \tag{4.1}$$

4.3. **The spectral results.** As in the previous cases, we start with a short description of the heuristics guiding our spectral results.

4.3.1. *The heuristics.* In Fig. 8, we draw γ_0 and γ_π, the connected components of Γ_R in one of the periodicity cells. According to the standard semi-classical heuristics, one expects each of these tori to give rise to a sequence of eigenvalues; these sequences are defined by Bohr-Sommerfeld like quantization conditions written in terms of the phases Φ_0 and Φ_π. The spectrum should be located near these quantized eigenvalues. The states interact through tunneling, and, as we now have two tori in a periodicity cell, they may resonate i.e. there may exist energies E satisfying both quantization conditions, that for γ_0 and that for γ_π. The tunneling at these resonant energies is quite different from the one at non resonant energies.

Let us first consider the case of a non resonant energy E. For the sake of definiteness, assume that E satisfies the quantization condition defined by Φ_0. Then, one expects that near E, one will find spectrum of $H_{z,\varepsilon}$ in an interval close to E; the width of this interval is given by the tunneling coefficients $t_{v,0}$ and t_h. At this energy, the states do not "see" the other array of tori, γ_π and its translates; nor do they "feel" the tunneling coefficient $t_{v,\pi}$. Essentially, one is in the situation of the "band edge" case with the "single" torus γ_0. In this case, one expects the nature of the spectrum to be determined by the ratio $t_{v,0}/t_h$. Of course, the situation is the same for an energy satisfying only the quantization condition given by Φ_π. So, the global picture for non resonant energies is that one has two sequences of (exponentially small) intervals, defined by Φ_0 and Φ_π. As the tunneling coefficients $t_{v,0}$ and $t_{v,\pi}$ are "independent" of each other, the nature of the spectrum on each of the sequences can be totally different. For instance, the spectrum can be absolutely continuous on one sequence of intervals and singular on the other one. In this case, one gets a sequence of mobility edges.

If the energy E is resonant for the two tori γ_0 and γ_π, then one may expect the tunneling in the horizontal direction to be stronger. We do not describe the tunneling regime in the present paper (see [8]); nevertheless, we get results for energies exponentially close to resonant energies. For such energies, we see that the parameter governing the nature of the spectrum is roughly $\max(t_{v,0}\cdot d_\pi(E), t_{v,\pi}\cdot d_0(E))/t_h$ where d_0 (resp. d_π) is the distance separating the energy one is considering from the nearest energy satisfying the quantization condition for γ_0 (resp. γ_π). So, the vertical tunneling becomes anomalously small; this can lead to a delocalization of the states associated to those energies.

4.3.2. *The spectral results.* We now assume that assumptions (H), (P) and (TIBM) hold.

Each of the functions $\Phi_0(E)$ and $\Phi_\pi(E)$ is positive, monotonically increasing on J, and its derivative does not vanish there. There are two real analytic functions $\check\Phi_0(E)$ and $\check\Phi_\pi(E)$ defined in a neighborhood of J and having the uniform asymptotics

$$\check\Phi_0(E) = \Phi_0(E) + o(\varepsilon), \quad \check\Phi_0(E) = \Phi_0(E) + o(\varepsilon). \tag{4.2}$$

These functions are the phases defining the quantization conditions. In J, consider the two sequences of points $E_0^{(l)}$ and $E_\pi^{(l)}$, $l \in \mathbb{N}$, defined by

$$\frac{1}{\varepsilon}\check\Phi_0(E_0^{(l)}) = \frac{\pi}{2} + \pi l, \quad \text{and} \quad \frac{1}{\varepsilon}\check\Phi_\pi(E_\pi^{(l)}) = \frac{\pi}{2} + \pi l, \quad l \in \mathbb{N}. \tag{4.3}$$

The number of these points is finite; we denote the minimal and the maximal values of l by $L_{0,\pi}^-$ and $L_{0,\pi}^+$. For sufficiently small ε, the points defined in (4.3) satisfy the inequalities

$$\begin{aligned}
\frac{1}{C}\varepsilon \le E_0^{(l)} - E_0^{(l-1)} \le C\varepsilon, \quad l = L_0^- + 1, \dots, L_0^+ \\
\frac{1}{C}\varepsilon \le E_\pi^{(l)} - E_\pi^{(l-1)} \le C\varepsilon, \quad l = L_\pi^- + 1, \dots, L_\pi^+
\end{aligned}$$

where C is a positive constant independent of ε.

Fix $\delta > 0$ small. Define $\mathcal{L}_0(\delta)$ to be the set of l from $\{L_0^-, \dots, L_0^+\}$ satisfying the inequalities

$$|E_\pi^{(l)} - E_0^{(l')}| \ge e^{\delta/\varepsilon}\left[t_h(E_0^{(l')}) + t_{v,0}(E_0^{(l')})\right] \qquad \forall\, L_0^- \le l' \le L_0^+. \tag{4.4}$$

The set $\mathcal{L}_\pi(\delta)$ is defined in an analogous way. The sets $\{E_0^{(l)}\}_{l\notin\mathcal{L}_0(\delta)}$ and $\{E_\pi^{(l)}\}_{l\notin\mathcal{L}_\pi(\delta)}$ form the set of resonant energies that one has to avoid. We also define

$$\mathcal{K}(\delta) = \left(\bigcup_{\substack{L_0^-\le l\le L_0^+ \\ l\notin\mathcal{L}_0(\delta)}} \left(E_0^{(l)} + e^{\delta/\varepsilon}\left\{t_h(E_0^{(l)}) + t_{v,0}(E_0^{(l)})\right\}\cdot[-1,1]\right)\right) \bigcup \left(\bigcup_{\substack{L_\pi^-\le l\le L_\pi^+ \\ l\notin\mathcal{L}_\pi(\delta)}} \left(E_\pi^{(l)} + e^{\delta/\varepsilon}\left\{t_h(E_\pi^{(l)}) + t_{v,\pi}(E_\pi^{(l)})\right\}\cdot[-1,1]\right)\right). \tag{4.5}$$

The set $\mathcal{K}(\delta)$ is just a neighborhood of the resonant energies.

Remark 4.2. As J is compact, the continuity and the non-vanishing of the functions S_h, $S_{v,0}$ and $S_{v,\pi}$ guarantee that, for some $\delta_0 > 0$, for all $E \in J$, one has

$$t_h(E) + t_{v,0}(E) + t_{v,\pi}(E) \le e^{-\delta_0/\varepsilon}.$$

Hence, for $0 < \delta < \delta_0$, the set $\mathcal{K}(\delta)$ consists of a union of $O(1/\varepsilon)$ exponentially small intervals.

For generic V, the set $\mathcal{L}_0(\delta)$ (resp. $\mathcal{L}_\pi(\delta)$) contains most of the indices from the set $\{L_0^-,\dots,L_0^+\}$ (resp. $\{L_\pi^-,\dots,L_\pi^+\}$). But, if V is even, then all $E_0^{(l)}$ and $E_\pi^{(l)}$ coincide and $\mathcal{L}_0(\delta) = \mathcal{L}_\pi(\delta) = \emptyset$!

We prove

Theorem 4.1. *Fix $\delta > 0$ sufficiently small. Then, for $\varepsilon > 0$ sufficiently small, there exists two collection of subintervals of J, say $(I_0^l)_{l\in\mathcal{L}_0}$ and $(I_\pi^l)_{l\in\mathcal{L}_\pi}$, such that,*

$$\Sigma \cap J \setminus \mathcal{K}(\delta) \subset \left(\bigcup_{l\in\mathcal{L}_0} I_0^l\right) \bigcup \left(\bigcup_{l\in\mathcal{L}_\pi} I_\pi^l\right).$$

For all $\alpha \in \{0,\pi\}$ and all $l \in \mathcal{L}_\alpha$, one has

- *the interval I_α^l contains $E_\alpha^{(l)}$;*
- *the length of I_α^l is exponentially small in ε (i.e. bounded by $e^{-C/\varepsilon}$ with some positive constant independent of I_α^l and ε);*
- *if $dN_\varepsilon(E)$ denotes the density of states measure of $H_{z,\varepsilon}$, then*

$$\int_{I_\alpha^l} dN_\varepsilon(E) = \frac{1}{2\pi}\varepsilon, \quad \forall I_\alpha^l \subset J\setminus\mathcal{K}(\delta).$$

Let us characterize the intervals I_α^l more precisely. For sake of definiteness, consider the case of $\alpha = \pi$. Then, the complement to the intervals I_π^l in $J\setminus\mathcal{K}(\delta)$ is described by the condition

$$\left|\cos\frac{\check\Phi_\pi(E)}{\varepsilon}\right| \ge C\left(t_{v,\pi}(E) + \frac{t_h(E)}{\sin\frac{\check\Phi_0(E)}{\varepsilon}}\right). \tag{4.6}$$

Fix $C > 0$ and a positive integer N. Inequality (4.6) implies, in particular, that, if E_π^l is situated outside $C\varepsilon^N$-neighborhood of the points $\{E_0^m\}$, then the measure of I_π^l admits the estimate

$$|I_\pi^l| \le \frac{C\varepsilon}{\Phi'_\pi(E_\pi^{(l)})}\left(t_{v,\pi}(E_\pi^{(l)}) + \frac{t_h(E_\pi^{(l)})}{\cos\frac{\check\Phi_0(E_\pi^{(l)})}{\varepsilon}}\right),$$

where C is a positive constant independent of I_π^l and ε. Note that, here, $|\cos\frac{\check\Phi_0(E_\alpha^{(l)})}{\varepsilon}| \ge \mathrm{Const}\,\varepsilon^N$.

The results on the location of the spectrum are quite similar to Theorem 3.1 except that in the present case one obtains two sequences of intervals containing spectrum. Each of these sequence is given by a

quantization condition defined by one of γ_0 and γ_π, the compact connected components of the real iso-energy surface (see Fig. 8). To get our result, we have to avoid the intervals in $\mathcal{K}(\delta)$; these correspond to the case when the quantization conditions for the two connected components of the real iso-energy surface give rise to the same energy. The source of the resonance effects is similar to one for the well known problem of resonant double wells (see e.g. [15] and references therein). We study these effects in [8].

Now, let us discuss the nature of the spectrum. Set

$$\lambda^0(E) = 2\left|\frac{t_{v,\pi}(E)}{t_h(E)}\cdot\nu\cdot\cos\left(\frac{\check\Phi_0}{\varepsilon}\right)+\frac{t_{v,0}(E)}{t_h(E)}\cdot\cos\left(\frac{\check\Phi_\pi}{\varepsilon}\right)\right|$$

where ν is defined after equation (3.5). Pick $\alpha\in\{0,\pi\}$. Notice that, on the intervals $I^l_\alpha\subset J\setminus\mathcal{K}(\delta)$,

$$\lambda^0(E) = 2\frac{t_{v,\alpha}(E)}{t_h(E)}\left|\cos\frac{\check\Phi_\beta}{\varepsilon}(E)\right|(1+o(1))+o(1), \tag{4.7}$$

where β is the index complementary to α in $\{0,\pi\}$, and $o(1)$ denotes terms exponentially small in ε.

For $c\geq 0$, define the set

$$J_c^- = \{E\in J;\ \varepsilon\cdot\log\lambda^0(E) < -c\}$$

We prove

Theorem 4.2. *Fix $c>0$. Pick $\sigma\in(0,1)$. Then there exists $D\subset(0,1)$ a set of Diophantine numbers such that*

- $$\frac{\operatorname{mes}(D\cap(0,\varepsilon))}{\varepsilon} = 1+o\left(\varepsilon^2 e^{-c\sigma/\varepsilon}\right)\ \text{when } \varepsilon\to 0.$$
- *For any ε small enough and $\varepsilon\in D$, each of the intervals $I_{l,\alpha}\subset J_c^-\setminus K(\delta)$ contains absolutely continuous spectrum, and, for these intervals,*

$$\frac{\operatorname{mes}(I_{l,\alpha}\cap\Sigma_{\rm ac})}{\operatorname{mes} I_{l,\alpha}} = 1+O(e^{-c\sigma/(2\varepsilon)}).$$

Here, Σ_{ac} is the absolutely continuous spectrum of $H_{z,\varepsilon}$.

Again fix c positive and let

$$J_c^+ = \{E\in J;\ \varepsilon\cdot\log\lambda^0(E) > c\}.$$

We prove

Theorem 4.3. *For sufficiently small ε, each of the intervals $I^l_\alpha\subset J_c^+\setminus K(\delta)$ contains only singular spectrum; moreover, in the interval I^l_α, one has*

$$\Theta(E) = \frac{\varepsilon}{2\pi}\log\lambda^0(E^{(l)}_\alpha)+o(\varepsilon).$$

Let us now comment on these results.

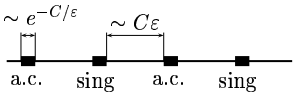

First, fix $C>0$ and a positive integer N. Assume that, in some energy region J_0 in J, the distances between the points $\{E^l_0\}$ and $\{E^l_\pi\}$ are larger than $C\varepsilon^N$. Then, on $I^l_\alpha\subset J_0$, one has $\left|\cos\frac{\check\Phi_\beta}{\varepsilon}\right|\geq$ Const ε^N, where β is complementary to α. This and formula (4.7) imply that, on I^l_α, the nature of the spectrum is determined the ratio $t_{v,\alpha}(E^l_\alpha)/t_h(E^l_\alpha)$. This simple observation leads to an unexpected effect. Assume, for example, that, on J_0, one also has

$$S_{v,\pi}(E)-S_h(E)>c \quad\text{and}\quad S_{v,0}(E)-S_h(E)<-c \tag{4.8}$$

for some fixed positive c. Then, inside J_0, the sequences of intervals corresponding to the quantization conditions for $\check\Phi_\pi$ and for $\check\Phi_0$ are of "opposite" spectral type, i.e. the spectrum on the intervals I^l_0 is singular, and it is essentially absolutely continuous on the intervals I^l_π. So, we get intertwined

sequences of exponentially small intervals of "opposite" spectral types. Notice also that, in this case, one gets $O(1/\varepsilon)$ spectral transitions.

Another new phenomenon occurs when one is close to the resonant case i.e. if the two quantization conditions give rise to roughly the same energy. Indeed, assume that on some energy interval $J_0 \subset J$, one has

$$S_h(E) - S_{v,0}(E),\ \ S_h(E) - S_{v,\pi}(E) \geq c \quad \text{and} \quad S_h(E) - 2\min_{\alpha}\{S_{v,\alpha}(E)\} \leq -c \tag{4.9}$$

with some positive fixed c. Fix δ positive, sufficiently small. Assume, moreover, that, on J_0, there exist two intervals $I_0^{(l)}$ and $I_\pi^{(k)}$ which are still non resonant (i.e. not in $\mathcal{K}(\delta)$), but are situated "near the boundary" of $K(\delta)$:

$$\operatorname{dist}(I_0^{(l)}, I_\pi^{(k)}) \sim e^{\delta/\varepsilon}(t_h(E_\pi^{(k)}) + t_{v,0}(E_\pi^{(k)}) + t_{v,\pi}(E_\pi^{(k)})). \tag{4.10}$$

Then, formula (4.7) imply that, in I_0^l and I_π^k, the spectrum will be absolutely continuous, though, on the neighboring intervals $I_\alpha^l \not\subset K(\delta)$, it will be singular. So, there are intervals where the spectral type changes due to resonance with the other quantization condition. This is a new type of spectral transition.

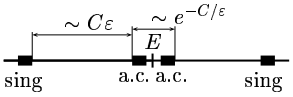

Remark 4.3. That the condition (4.10) will be satisfied for some energies is clear as one can vary both the energy and the adiabatic parameter ε.

4.4. **The asymptotics of the monodromy matrix.** Theorem 1.2 holds for J, a compact energy interval satisfying (TIBM). Under the hypothesis (TIBM) and (P), the monodromy matrix admits the representation (0.8). As in section 3.4, one introduces $F(E)$, the effective spectral parameter, and $\lambda(E)$, the effective coupling constant. These two objects play the same role as in the "band edge" case.

Fix C_1 positive. Now, one proves that, if $\operatorname{Re} E \in J$, $|\operatorname{Im} E| \leq C_1$, then

$$\begin{aligned} F(E) &= 4e^{\frac{S_h(E)}{\varepsilon}+o(1)} \cos\left(\frac{\check\Phi_\pi}{\varepsilon}\right)\cos\left(\frac{\check\Phi_0}{\varepsilon}\right) + O(1) + R_F, \\ \lambda(E) &= 2\left|\frac{t_{v,\pi}(E)}{t_h(E)}\cdot\nu\cdot\cos\frac{\check\Phi_0}{\varepsilon}\,(1+o(1)) + \frac{t_{v,0}(E)}{t_h(E)}\cdot\cos\frac{\check\Phi_\pi}{\varepsilon}\,(1+o(1))\right| + O(\max_\alpha\{t_{v,\alpha}\}) + R_\lambda, \end{aligned} \tag{4.11}$$

where R_F and R_λ, the reminder terms, are of the form

$$O\left(e^{-C/\varepsilon}\,\frac{\min_\alpha(t_{v,\alpha})}{t_h}\,\left[\,\left|\cos\frac{\check\Phi_0}{\varepsilon}\right| + \left|\cos\frac{\check\Phi_\pi}{\varepsilon}\right|\,\right] + \frac{t_{v,0}t_{v,\pi}}{t_h}\right). \tag{4.12}$$

The analysis of the traces of the monodromy matrix is summed up in Fig. 10.

Remark 4.4. As in the "band edge" case, the proof the asymptotics for $F(E)$ and $\lambda(E)$ is based on a factorization of the monodromy matrix in a product of two matrices 1-periodic in z and having determinants independent of z. The factorization again is described by (3.7) and, again, $\det P = \det Q$. But, now, the determinants are bounded away from zero by a constant independent of ε. The representations (3.8) still hold true. Under the assumptions (H), (O) and (TIBM), one obtains

$$\begin{aligned} \alpha_0 &= \frac{1}{\sqrt{t_h}}e^{i\frac{\Phi_0}{2\varepsilon}+i\frac{\Phi_\pi}{2\varepsilon}+A_0+o(1)}, \quad \beta_0 = \frac{1}{\sqrt{t_h}}e^{i\frac{\Phi_0}{2\varepsilon}-i\frac{\Phi_\pi}{2\varepsilon}+B_0+o(1)}, \\ \gamma_0 &= \frac{1}{\sqrt{t_h}}e^{-i\frac{\Phi_\pi}{2\varepsilon}-i\frac{\Phi_0}{2\varepsilon}+C_0+o(1)}, \quad \delta_0 = \frac{1}{\sqrt{t_h}}e^{i\frac{\Phi_\pi}{2\varepsilon}+i\frac{\Phi_0}{2\varepsilon}+D_0+o(1)}, \\ \alpha_1 &= \alpha_0\cdot t_{v,\pi}\cdot e^{-i\frac{\Phi_0}{\varepsilon}+A_1+o(1)}, \quad \beta_1 = \beta_0\cdot t_{v,0}\cdot e^{-i\frac{\Phi_0}{\varepsilon}+B_1+o(1)}, \\ \gamma_{-1} &= \gamma_0\cdot t_{v,\pi}\cdot e^{i\frac{\Phi_\pi}{\varepsilon}-\frac{2i\pi^2}{\varepsilon}+C_1+o(1)}, \quad \delta_1 = \delta_0 t_{v,\pi}e^{-i\frac{\Phi_\pi}{\varepsilon}+\frac{2i\pi^2}{\varepsilon}+D_1+o(1)} \end{aligned}$$

with the phases and actions defined in section 4.1; $A_{0,1}$, $B_{0,1}$, $C_{0,1}$, $D_{0,1}$ are constants.

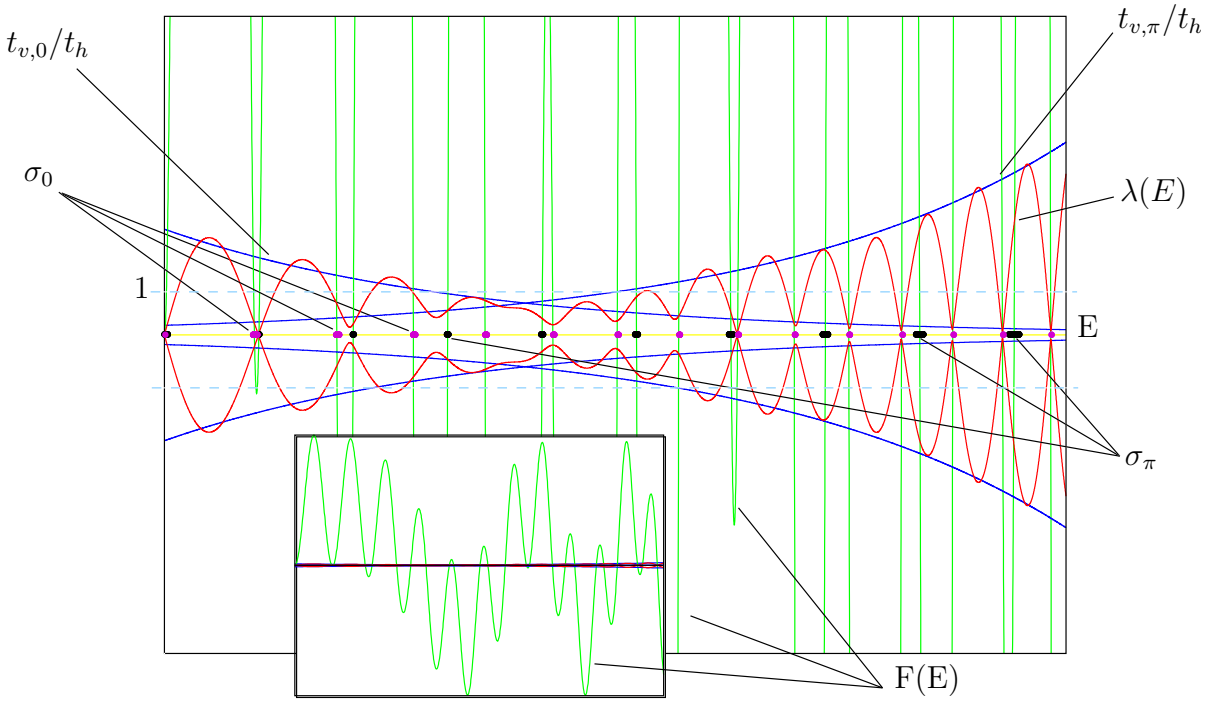

Figure 10: Analysis of the traces of monodromy matrix in the "two interacting band" case

References

[1] J. Avron and B. Simon. Almost periodic Schrödinger operators, II. the integrated density of states. *Duke Mathematical Journal*, 50:369–391, 1983.

[2] V. Buslaev. Adiabatic perturbation of a periodic potential. *Theor. Mat. Fiz.*, 58:223–243, 1984 (in Russian).

[3] V. Buslaev and A. Fedotov. Bloch solutions of difference equations. *St Petersburg Math. Journal*, 7:561–594, 1996.

[4] H. Cycon, R. Froese, W. Kirsch, and B. Simon. *Schrödinger Operators*. Springer Verlag, Berlin, 1987.

[5] E. I. Dinaburg and Ja. G. Sinaĭ. The one-dimensional Schrödinger equation with quasiperiodic potential. *Funkcional. Anal. i Priložen.*, 9(4):8–21, 1975.

[6] L. H. Eliasson. Floquet solutions for the 1-dimensional quasi-periodic Schrödinger equation. *Communications in Mathematical Physics*, 146:447–482, 1992.

[7] A. Fedotov and F. Klopp. On complex tunneling and Lyapunov exponents for adiabatic quasi-periodic Schrödinger equation on the real line. In progress.

[8] A. Fedotov and F. Klopp. Resonant microlocal wells for adiabatic quasi-periodic Schrödinger equation on the real line. In progress.

[9] A. Fedotov and F. Klopp. A complex WKB method for adiabatic problems. *Asymptotic Analysis*, 27:219–264, 2001.

[10] A. Fedotov and F. Klopp. On the absolutely continuous spectrum of one dimensional quasi-periodic Schrödinger operators in the adiabatic limit. Preprint, Université Paris-Nord, 2001. Mathematical Physics Preprint Archive Preprint 01-224 http://www.ma.utexas.edu/mp_arc-bin/mpa?yn=01-224.

[11] A. Fedotov and F. Klopp. Anderson transitions for a family of almost periodic Schrödinger equations in the adiabatic case. *Comm. Math. Phys.*, 227(1):1–92, 2002.

[12] A. Fedotov and F. Klopp. Geometric tools for the adiabtic complex WKB method with applications to the monodromy matrix for adiabatic quasi-periodic Schrödinger operators. In progress.

[13] A. Fedotov and F. Klopp. On the singular spectrum of one dimensional quasi-periodic Schrödinger operators in the adiabatic limit. Mathematical Physics Preprint Archive Preprint 02-69 http://www.ma.utexas.edu/mp_arc-bin/mpa?yn=02-69.

[14] A. Fedotov and F. Klopp. The phase diagram for one dimensional quasi-periodic Schrödinger operators in the adiabatic limit. In progress.

[15] B. Helffer and J. Sjöstrand. Multiple wells in the semi-classical limit I. *Communications in Partial Differential Equations*, 9:337–408, 1984.

[16] M. Herman. Une méthode pour minorer les exposants de Lyapounov et quelques exemples montrant le caractère local d'un théorème d'Arnol'd et de Moser sur le tore de dimension 2. *Comment. Math. Helv.*, 58(3):453–502, 1983.

[17] T. Janssen. Aperiodic Schrödinger operators. In R. Moody, editor, *The Mathematics of Long-Range Aperiodic Order*, pages 269–306. Kluwer, 1997.
[18] Y. Last and B. Simon. Eigenfunctions, transfer matrices, and absolutely continuous spectrum of one-dimensional Schrödinger operators. *Invent. Math.*, 135(2):329–367, 1999.
[19] L. Pastur and A. Figotin. *Spectra of Random and Almost-Periodic Operators*. Springer Verlag, Berlin, 1992.
[20] J. Puig. Reducibility of linear equations with quasi-periodic coefficients. A survey. Mathematical Physics Preprint Archive Preprint 02-246 http://www.ma.utexas.edu/mp_arc-bin/mpa?yn=02-246.
[21] E. Sorets and T. Spencer. Positive Lyapunov exponents for Schrödinger operators with quasi-periodic potentials. *Comm. Math. Phys.*, 142(3):543–566, 1991.

(Alexander Fedotov) Departement of Mathematical Physics, St Petersburg State University, 1, Ulianovskaja, 198904 St Petersburg-Petrodvoretz, Russia
E-mail address: fedotov@mph.phys.spbu.ru

(Frédéric Klopp) Département de Mathématique, Institut Galilée, U.M.R 7539 C.N.R.S, Université de Paris-Nord, Avenue J.-B. Clément, F-93430 Villetaneuse, France
E-mail address: klopp@math.univ-paris13.fr